J Bone Miner Metab (2013) 31:26–33
DOI 10.1007/s00774-012-0380-2

ORIGINAL ARTICLE

Clinically applicable antianginal agents suppress osteoblastic transformation of myogenic cells and heterotopic ossifications in mice

Ryuichiro Yamamoto · Masaki Matsushita · Hiroshi Kitoh · Akio Masuda · Mikako Ito · Takenobu Katagiri · Tatsushi Kawai · Naoki Ishiguro · Kinji Ohno

Received: 7 March 2012 / Accepted: 18 July 2012 / Published online: 24 August 2012

Abstract Fibrodysplasia ossificans progressiva (FOP) is a rare autosomal dominant disorder characterized by progressive heterotopic ossification. FOP is caused by a gain-of-function mutation in *ACVR1* encoding the bone morphogenetic protein type II receptor, ACVR1/ALK2. The mutant receptor causes upregulation of a transcriptional factor, Id1. No therapy is available to prevent the progressive heterotopic ossification in FOP. In an effort to search for clinically applicable drugs for FOP, we screened 1,040 FDA-approved drugs for suppression of the *Id1* promoter activated by the mutant ACVR1/ALK2 in C2C12 cells. We found that that two antianginal agents, fendiline hydrochloride and perhexiline maleate, suppressed the *Id1* promoter in a dose-dependent manner. The drugs also suppressed the expression of native *Id1* mRNA and alkaline phosphatase in a dose-dependent manner. Perhexiline but not fendiline downregulated phosphorylation of Smad 1/5/8 driven by bone morphogenetic protein (BMP)-2. We implanted crude BMPs in muscles of ddY mice and fed them fendiline or perhexiline for 30 days. Mice taking perhexiline showed a 38.0 % reduction in the volume of heterotopic ossification compared to controls, whereas mice taking fendiline showed a slight reduction of heterotopic ossification. Fendiline, perhexiline, and their possible derivatives are potentially applicable to clinical practice to prevent devastating heterotopic ossification in FOP.

Keywords Fibrodysplasia ossificans progressiva · Heterotopic ossification · Perhexiline maleate · Fendiline hydrochloride · C2C12 myogenic cells

Electronic supplementary material The online version of this article (doi:10.1007/s00774-012-0380-2) contains supplementary material, which is available to authorized users.

R. Yamamoto · M. Matsushita · A. Masuda · M. Ito · K. Ohno (✉)
Department of Neurogenetics, Center for Neurological Diseases and Cancer, Nagoya University Graduate School of Medicine, 65 Tsurumai, Showa-ku, Nagoya 466-8550, Japan
e-mail: ohnok@med.nagoya-u.ac.jp

R. Yamamoto · M. Matsushita · H. Kitoh · N. Ishiguro
Department of Orthopaedic Surgery, Nagoya University Graduate School of Medicine, Nagoya, Japan

T. Katagiri
Division of Pathophysiology, Research Center for Genomic Medicine, Saitama Medical University, Saitama, Japan

T. Kawai
Department of Dental and Material Science, Aichi-Gakuin University School of Dentistry, Nagoya, Japan

Introduction

Fibrodysplasia ossificans progressiva (FOP) is a rare autosomal dominant disorder characterized by progressive heterotopic ossification (HO) in connective tissues, especially in skeletal muscles [1]. In FOP, HO tends to develop after physical trauma [2], surgical treatment including biopsy [3, 4], and intramuscular injection [5, 6]. Ectopic bone formation similar to that observed in FOP is induced by implantation of bone morphogenetic proteins (BMPs) into muscle tissue [7, 8]. BMPs bind to and activate activin A receptor type I (ACVR1/ALK2), which induces phosphorylation of Smad 1/5/8. Phosphorylated Smads are translocated into nuclei to facilitate expression of various genes. Among them, Id1 is a key molecule that leads to osteoblastic differentiation. Shore and colleagues first reported an autosomal dominant c.617G>A mutation predicting R206H in the GS domain of ACVR1/ALK2 [9].

The R206H mutation constitutively activates BMP-independent phosphorylation of Smad 1/5/8. FOP is currently treated with conventional anti-inflammatory or anti-osteogenic agents including corticosteroids, non-steroidal anti-inflammatory drugs (NSAIDs) [10], COX-2 inhibitors [11], bisphosphonates [4, 12, 13], mast cell inhibitors [14], radiation therapy [15], and bone marrow transplantation along with immunosuppressants [16], but without discernible effects [17]. Recently, in-vitro and in-vivo effects of dorsomorphin [18] and LDN-193189 [19], inhibitors of the ACVR1/ALK2 receptor, have been reported in cultured cells and mice. Similarly, CD1530, an agonist of nuclear retinoic acid receptor-γ, prevents HO in FOP model mice [20]. None of these compounds, however, has been applied in clinical practice. Pharmaceutical companies do not invest a large amount of research budget in developing novel therapeutic agents for orphan diseases including FOP. A promising alternative for orphan diseases is a drug repositioning strategy, in which a drug currently used for patients with a specific disease is applied to another disease [21, 22]. The advantage of this strategy is that the identified drug can be readily applied to clinical practice, because the optimal doses and adverse effects are already established. We thus screened 1,040 FDA-approved drugs for suppression of the mutant ACVR1/ALK2-activated *Id1* promoter [23] in C2C12 mouse myogenic cells, and found that two antianginal agents, fendiline hydrochloride and perhexiline maleate, potentially ameliorate HO in model cells and mice.

Materials and methods

Screening of 1,040 FDA-approved compounds in C2C12 cells

We purchased a panel of 1,040 US FDA-approved drugs (NINDS-2, MicroSource Discovery Systems). The names of the 1,040 compounds are available at http://www.msdiscovery.com/usdrugs.html. Mouse C2C12 myoblasts were cultured in Dulbecco's Modified Eagle's Medium (DMEM) containing 15 % fetal bovine serum (FBS) without decomplementation. At ~70 % confluency in a 10-cm dish, C2C12 cells were transiently transfected with IdWT4F-Luc that carried the firefly luciferase cDNA driven by the SV-40 promoter and four copies of a BMP-responsive 29-bp enhancer element [23]. Cells were also transfected with human ALK2-R206H that carried a mutant ALK2 driven by the EF1α promoter, as well as with phRL-TK expressing Renilla luciferase (Promega). The transfection reagent included 20 μg of ALK2-R206H, 2 μg of IdWT4F-Luc, 0.4 μg of phRL-TK, and 60 μl of Lipofectamine 2000 (Invitrogen) for a 10-cm dish according to the manufacturer's instructions. At 1 h after incubation with the transfection reagent, the medium was changed to DMEM containing 2.5 % FBS. At 24 h after transfection, cells were split into three 96-well plates containing 10 μM of each compound and 2 % DMSO, and were incubated for an additional 24 h. We screened the effect of each compound by quantifying the firefly luciferase activity normalized for the Renilla luciferase activity using the Dual-Luciferase Reporter Assay System (Promega) in the Luminoskan Ascent (Thermo Scientific). The relative luciferase activity was also normalized to that in the absence of any compound. To analyze a dose–response effect, we added up to 20 μM of fendiline and up to 10 μM of perhexiline maleate.

Real-time RT-PCR to quantify *Id1*, *Id2*, and *Id3* mRNAs

For quantifying *Id1*, *Id2*, and *Id3* mRNAs, we plated C2C12 cells in DMEM containing 10 % decomplemented FBS overnight, and changed the media to DMEM containing 2.5 % FBS in the presence of variable concentrations of fendiline hydrochloride (Sigma) or perhexiline maleate (MicroSource Discovery Systems) with or without 100 ng/ml BMP-2 (Peprotech). After incubation for 6 h, total RNA was isolated from C2C12 cells using the GenElute Mammalian Total RNA kit (Sigma). We synthesized cDNA using the ReverTra Ace reverse transcriptase (Toyobo) and Oligo-dT (Invitrogen). PCR primers were 5′-GCTGGTACT CAGGGCTCAAG-3′ and 5′-GCCGTTCAGGGTGCTG-3′ for *Id1*; 5′-CTGGACTCGCATCCCACTAT-3′ and 5′-GCT ATCATTCGACATAAGCTCAGA-3′ for *Id2*; 5′-ACTCA GCTTAGCCAGGTGGA-3′ and 5′-TCAGTGGCAAAAG CTCCTCT-3′ for *Id3*; and 5′-ATTCACCCCCACTGAG ACTG-3′ and 5′-TGCTATTTCTTTCTGCGTGC-3′ for a gene for β_2-microglobulin. We quantified mRNA using the SYBR Green SuperMix (Invitrogen) in Mx3000P (Stratagene) in triplicate. Expression levels of *Id1*, *Id2*, and *Id3* were normalized to that of β_2-microglobulin.

Alkaline phosphatase activity to estimate osteoblastic transformation

C2C12 cells were split into 96-well plates in DMEM with 2.5 % decomplemented FBS in the presence 0.025, 0.05, 0.1, 0.2, 0.5, 1, 2, and 5.0 μM fendiline hydrochloride or perhexiline maleate with or without 100 ng/ml BMP-2 (Peprotech). After culturing cells for 5 days, we removed the culture media and added 25 μl of Tris-buffered saline (pH 7.5) containing 1 % Triton X-100 and 50 μl *p*-nitrophenyl-phosphate liquid substrate (N7353, Sigma). After the reaction mixture developed a yellowish color in 15–60 min at room temperature, the reaction was terminated by adding 50 μl of 3 M NaOH and the absorbance at 405 nm was measured in Sunrise Remote R (Tecan) [24, 25].

Western blotting

We added DMEM with 2.5 % decomplemented FBS to C2C12 cells in a 6-well plate and incubated for 6 h. We then added 5 μM of fendiline hydrochloride, perhexiline maleate, or dorsomorphin (Sigma), and incubated for 30 min. We harvested cells by directly adding 600 μl of HEPES–KOH buffer (10 mM HEPES pH 7.8, 10 mM KCl, 0.1 mM EDTA, 1 mM DTT, 2 μg/ml aprotinin, 0.5 mM PMSF, 0.1 % NP-40) and incubated on ice for 20 min. After sonication, samples were centrifuged at 14,000*g* for 5 min. The supernatants were analyzed by Western blotting with anti-Smad 1 (sc-81378, Santa Cruz) and anti-phospho-Smad 1/5/8 (#9511, Cell Signaling) antibodies.

Transplantation of crude BMPs into mouse muscle and microCT analysis

All animal studies were approved by the Animal Care and Use Committee of the Nagoya University Graduate School of Medicine. We purchased 6 week-old male ddY mice from Japan SLC, Inc. Eighteen mice were divided into three groups: control, perhexiline, and fendiline. Each compound (100 mg) was mixed in 100 g of food powder, and the mice were fed ad libitum. The mice started taking each compound 1 day before surgery. Mice (30 g) took ~3 g of food per day, which was equivalent to ~3 mg of each compound. Crude BMPs were prepared by freezing and pulverizing fresh bovine cortical bone followed by demineralization with 0.6 M HCl for 72 h. The preparation was washed with 2 M $CaCl_2$ and with 0.5 M EDTA, and was extracted with a buffer containing 6 M urea, 0.5 $CaCl_2$, 1 mM *N*-ethylmaleimide, and 1 mM benzamidine [26]. Crude BMPs (5 mg) were packed in a gelatin capsule (length 11.1 mm, diameter 4.91 mm, and volume 0.13 ml) and were implanted in the muscle pouch of the left posterior region of the thigh under diethyl ether anesthesia, as previously described [8]. On day 30 after the surgery, we obtained transverse micro-computed tomography (microCT) images of the lower pelvis and hindlimbs at 90 kV and 88 μA at 50-μm resolution. We quantified HO using the 3D-BON software (Ratoc). On day 30, we also measured serum ALT, AST, BUN, creatine, and albumin, and found no abnormalities in any group.

Results

Screening of 1,040 FDA-approved drugs for inhibition of osteoblastic differentiation of C2C12 cells

To search for a drug that ameliorates HO in FOP, we transiently introduced the wild-type or mutant ACVR1/ALK2 carrying R206H into C2C12 mouse myogenic cells along with the firefly luciferase cDNA driven by the mouse *Id1* promoter. We also introduced the TK promoter-driven Renilla luciferase cDNA (phRL-TK) as a control. We first confirmed that the mutant ACVR1/ALK2 increases the firefly luciferase activity 8.4-fold (wild-type, 139 ± 82 arbitrary units; R206H, 1,168 ± 311 arbitrary units, mean ± SD of three experiments). We then added 10 μM of 1,040 FDA-approved chemical compounds to C2C12 cells at 24 h after transfection and incubated for an additional 24 h. We omitted compounds that compromised cell viability by examining cells under the microscope. We repeated the assays three times and chose 100 best compounds. With the 100 compounds, we further repeated the assays three or more additional times. We also analyzed an effect on the CMV-driven firefly luciferase activity of the 100 compounds, and omitted 10 compounds that decreased the control firefly luciferase activity to less than 80 %. After the first and second rounds of screening, we chose 10 best compounds that consistently exhibited beneficial effects (Table 1).

Table 1 The ten most effective compounds

Compound	Normalized F/R[a]	Pharmacological effect
Fendiline hydrochloride	0.238 ± 0.217	Ca^{2+} channel blocker
6,4′-Dihydroxyflavone	0.325 ± 0.206	Antihemorrhagic
Polymyxin B sulfate	0.619 ± 0.248	Antibacterial
Ethaverine hydrochloride	0.637 ± 0.264	Antispasmodic
Phenylephrine hydrochloride	0.658 ± 0.268	α_1-Adrenergic agonist
Rofecoxib	0.679 ± 0.116	COX2 inhibitor
Hexachlorophene	0.687 ± 0.233	Topical disinfectant
Flutamide	0.752 ± 0.223	Antiandrogen
1,8-Dihydroxyanthraquinone	0.780 ± 0.141	Laxative
Vidarabine	0.783 ± 0.127	Antiviral

[a] Normalized F/R represents the mean and SE ($n = 9$) of the firefly luciferase activity driven by the *Id1* promoter normalized for the cotransfected Renilla luciferase activity and also for no compound

Dose-dependent effects of the identified drugs in C2C12 cells

We next examined dose-dependent effects by adding 0.0, 0.1, 0.2, 0.5, 1.0, 2.0, 5.0, 10.0, and 20.0 μM of the 10 compounds. Among them, fendiline hydrochloride showed the most consistent and promising dose-dependent suppression of the *Id1* promoter activity (Fig. 1a). As fendiline is a calcium channel blocker, we examined dose-dependent effects of the other eight calcium channel blockers included in the initial drug panel, although most of them exhibited

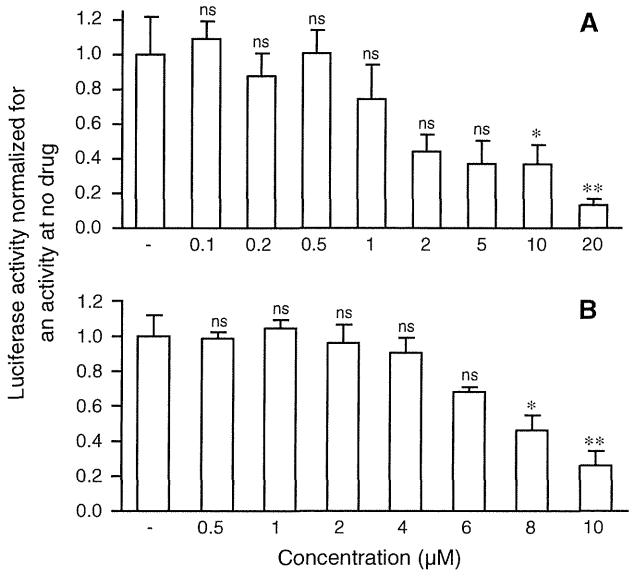

Fig. 1 Dose–response effects of fendiline hydrochloride (**a**) and perhexiline maleate (**b**) on *Id1* promoter activities. The mouse *Id1* promoter fused with the firefly luciferase cDNA is introduced into C2C12 cells along with Renilla luciferase cDNA driven by the TK promoter. The ratio of the firefly/Renilla luciferase activities is normalized to that without any compound. *Bars* represent the mean and SE of three experiments. $*P < 0.05$, $**P < 0.01$, and not significant (ns) compared to no drug

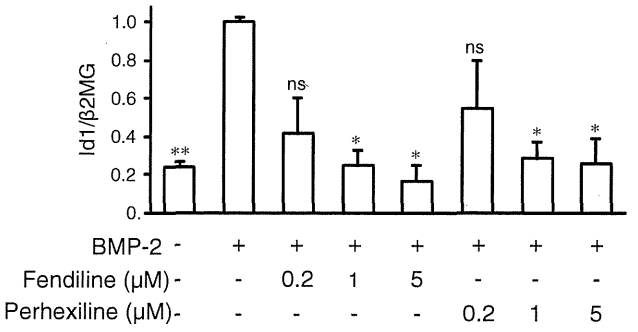

Fig. 2 Real time RT-PCR of the native *Id1* gene in C2C12 cells in the presence of variable concentrations of fendiline hydrochloride and perhexiline maleate. Values are normalized to the expression level of β_2-microglobulin (*b2MG*) and also to that with 100 ng/ml of BMP-2 alone. *Bars* represent the mean and SE of three experiments. $*P < 0.05$, $**P < 0.01$, and not significant (ns) compared to BMP-2(+) but without a drug

no effect at 10 μM in the screening experiments. We found that another calcium channel blocker, perhexiline maleate, also had a dose-dependent suppressive effect on the *Id1* promoter activity (Fig. 1b).

Fendiline hydrochloride and perhexiline maleate suppress native *Id1* mRNA and osteoblastic transformation in C2C12 cells

We then examined effects of fendiline and perhexiline on the expression of the native *Id1* gene in C2C12 cells. We added 0.0, 0.2, 1.0, and 5.0 μM of the compounds to nascent C2C12 cells in the presence or absence of 100 ng/ml BMP-2. We harvested C2C12 cells at 24 h after adding each compound and quantified *Id1* mRNA by real-time RT-PCR. Both compounds suppressed the expression levels of the native *Id1* mRNA in a dose-dependent manner (Fig. 2). We also examined effects of fendiline and perhexiline on the expression of the native *Id2* and *Id3* genes in C2C12 cells, but found no effects (Supplementary Fig. 1). We could not quantify the native osteocalcin mRNA levels in response to the two compounds in C2C12 cells, because the expression levels were too low to be quantified by real-time RT-PCR even at seven days after differentiation.

We additionally examined effects of fendiline and perhexiline on the BMP-2-induced osteoblastic differentiation of C2C12 cells by measuring the alkaline phosphatase activity. Alkaline phosphatase activity was efficiently induced in 5 days after adding 100 ng/ml BMP-2, and was suppressed by both compounds in a dose-dependent manner (Fig. 3).

We also examined by Western blotting whether fendiline and perhexiline suppress the BMP-SMAD pathway in C2C12 cells. We found that fendiline did not suppress phosphorylation of Smad 1/5/8, whereas perhexiline suppressed the phosphorylation to 62.9 % of the control (Fig. 4). The extent of suppression, however, was not as great as that achieved by dorsomorphin, a previously reported inhibitor of the ACVR1/ALK2 receptor [18, 19, 27].

Fendiline hydrochloride slightly and perhexiline maleate moderately inhibit heterotopic ossification of mice muscles implanted with crude BMPs

We examined the effects of fendiline and perhexiline on HO in 6-week-old ddY mice. The mice were fed with ~3 mg of each compound per day on day 0. Assuming that the compound was completely absorbed and evenly dissolved in 60 % body water, the serum concentration was expected to be 167 mg/kg. As 60-kg patients take 100–200 mg of perhexiline and 300 mg of fendiline in clinical practice, the serum concentrations are predicted to be 2.8–5.6 and 8.3 mg/kg, respectively. Thus, the mice were given 30–60 times more perhexiline and 20 times more fendiline compared to patients. Ten-fold or more higher amounts of chemical compounds are commonly used in mouse experiments, and we also chose the higher dosages. On day 1, a total of 18 mice taking either control, perhexiline, or fendiline were implanted with 5 mg of crude BMP extracts packed in a gelatin capsule. Two mice on perhexiline and three mice on fendiline died within

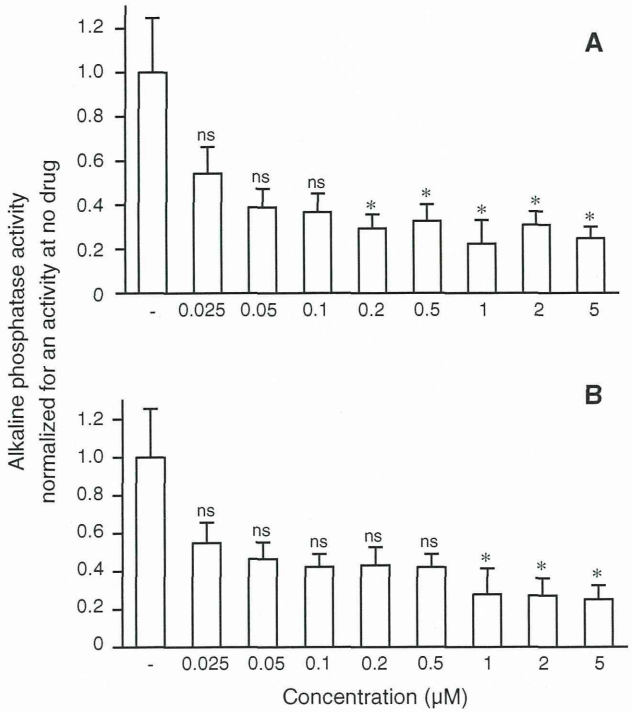

Fig. 3 Alkaline phosphatase activities of C2C12 cells in the presence of variable concentrations of fendiline hydrochloride (**a**) and perhexiline maleate (**b**). C2C12 cells are subject to osteoblastic differentiation by 100 ng/ml of BMP-2. Values are normalized to that with 100 ng/ml of BMP-2 alone. *Bars* represent the mean and SE of three experiments. $*P < 0.05$ and not significant (ns) compared to no drug

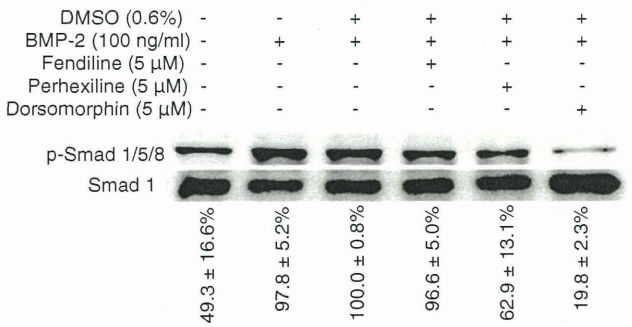

Fig. 4 Immunoblots of phosphorylated Smad 1/5/8 and Smad 1 of C2C12 cells at 30 min after adding 100 ng/ml BMP-2. Representative blots of three experiments are demonstrated. Values represent the mean and SE of relative intensities of phosphorylated Smad 1/5/8 of three experiments

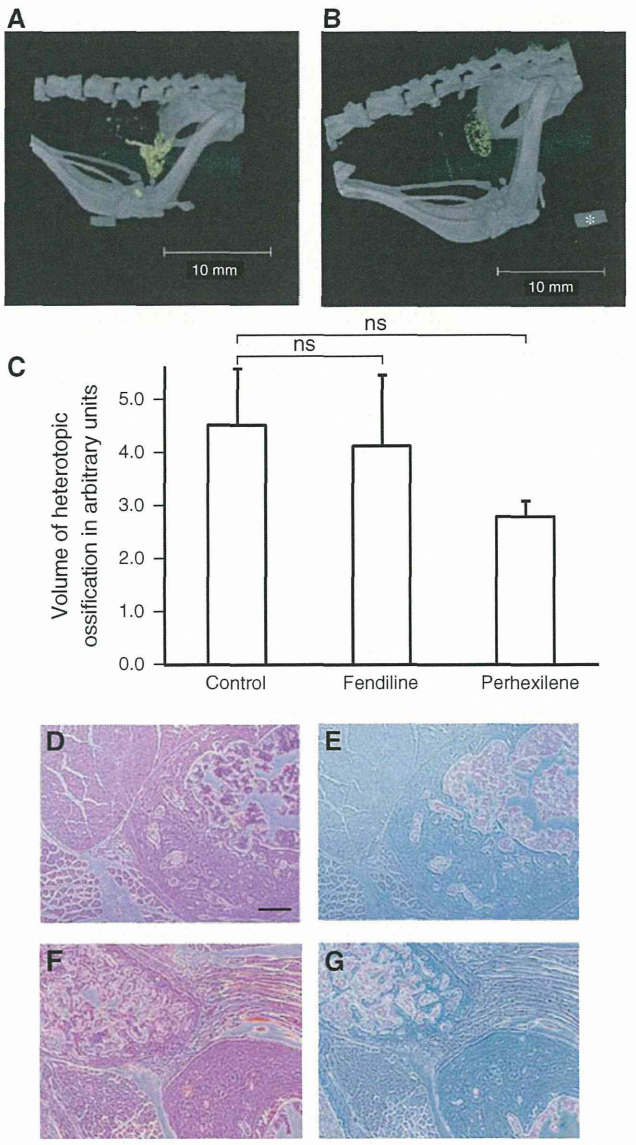

Fig. 5 MicroCT analysis of heterotopic ossifications in mouse muscles implanted with a capsule of crude BMP. Representative 3D microCT images of lower pelvis and hindlimbs of control mice (**a**) and perhexiline-treated mice (**b**). Heterotopic ossifications are *highlighted*. An *asterisk* indicates a phantom. (**c**) Volumetric analysis of heterotopic ossifications. *Bars* represent the mean and SE of three to three to six mice (see "Materials and methods"). H&E (**d**, **f**) and Alcian Blue (**e**, **g**) staining of heterotopic ossifications in muscles of control mice (**d**, **e**) and perhexiline-treated mice (**f**, **g**). *Bar* 200 μm, *ns* not significant

1 day after surgery. The mice started taking perhexiline or fendiline 1 day before surgery to ensure that the drug concentrations became high enough to prevent BMP-induced HO, but the drugs might have enhanced surgical stress, which culminated in the death of some mice. On day 30, we quantified volumes of HO using microCT (Fig. 5). Mice taking perhexiline showed 38.0 ± 6.1 % (mean and SE, $n = 4$) reduction of the HO volume compared to controls ($n = 6$). Highly variable HO volumes among the mice, however, prevented us from showing statistical significance with Student's t test. Mice taking fendiline ($n = 3$) showed a slight reduction of the HO volumes but again without statistical significance. Hematoxylin/eosin (H&E) and Alcian Blue staining of HO in muscles revealed no histological difference between the control and perhexiline-treated mice (Fig. 5d, e, f, g).

Discussion

Drug repositioning

The drug repositioning strategy, in which a panel of preapproved drugs is used to search for therapeutic modalities, was first proposed and funded by NINDS for neurodegenerative diseases [21, 22]. Off-label effects of several preapproved compounds have been reported, mostly for neurodegenerative diseases [28–31]. In the current studies, we screened 1,040 FDA-approved drugs and found that two antianginal agents, fendiline hydrochloride and perhexiline maleate, suppress the *Id1* promoter and osteogenic differentiation of C2C12 myogenic cells, and also suppress HO in model mice.

Fendiline hydrochloride

Fendiline hydrochloride is an open state blocker of L-type calcium channel for treating hypertension and angina pectoris [32, 33]. Fendiline is available for clinical practice in Germany. Fendiline also works as a calmodulin antagonist [34] and as a calcimimetic that stimulates the calcium-sensing receptor on the cell membrane [35–37]. Fendiline increases intracellular Ca^{2+} levels in various cell types [38–41], which is mediated by facilitating release of endoplasmic Ca^{2+} in an IP3-independent manner and also by triggering entry of extracellular Ca^{2+} [40]. Increased intracellular concentration of Ca^{2+} inhibits osteoblast formation, which is likely mediated by modulating a balance between adenylate cyclase and phosphodiesterase IV [42, 43]. Effects of fendiline on HO may be attributed to this mechanism. Calcimimetics stimulate the calcium-sensing receptor, which has the same effect as increasing extracellular Ca^{2+} concentration for the receptor-expressing cells. In clinical practice, cinacalcet, a calcimimetic, is used for secondary hyperparathyroidism associated with hemodialysis and for functional hyperparathyroidoma to ameliorate soft tissue calcification [44–46]. Stimulation of the calcium-sensing receptor of myoblasts and muscle tissue by fendiline may partly contribute to suppression of osteoblastic differentiation of muscle cells.

Perhexiline maleate

Perhexiline maleate was introduced for clinical use in the 1970s as a prophylactic antianginal drug and widely used for treatment of stable angina in the United States and other countries. The use of perhexiline, however, declined in the 1980s as adverse drug reactions surfaced [47]. Major adverse events included peripheral neuropathy, hepatic damage including cirrhosis, hypoglycemia, and weight loss. Further studies identified that *CYP2D6* polymorphisms determine the drug metabolism rate, which leads to significantly different plasma concentrations and elimination half-lives [48]. Due to the adverse effects, perhexiline maleate was essentially discontinued in the United States in 1976 [47, 49, 50]. In 1986, however, Horowitz and colleagues reported that maintaining the plasma concentration of perhexiline between 0.15 and 0.60 mg/L enables safe use of the drug without compromising efficiency [51, 52]. Perhexiline is now prescribed for refractory angina in Australia and New Zealand, as well as in Europe, in conditions where plasma concentrations are regularly monitored to ensure safety and efficacy [53]. Plasma concentrations of perhexiline are indeed routinely measured by Dr. John D. Horowitz at Queen Elizabeth Hospital, Woodville, Australia for essentially all the patients taking perhexiline.

Perhexiline has a weak L-type calcium channel blocking effect [54]. In addition, perhexiline inhibits carnitine palmitoyl transferase I (CPT-I) [55]. CPT-I is located on the outer mitochondrial membrane and is responsible for transferring an acyl moiety of long-chain free fatty acids (FFAs) into mitochondria. Inhibition of CPT-I precipitates a shift of mitochondrial energy source from FFAs to carbohydrate. As the oxidation of carbohydrates requires 10–15 % less oxygen than that of FFAs, cardiac function is improved. In addition, partial inhibition of FFA oxidation decreases lactate by facilitating oxidation of pyruvate, which increases pH of heart muscles and improves contractile function during ischemia [56]. Additionally, perhexiline potentiates sensitivity of platelets to nitric oxide, which is expected to inhibit platelet aggregation in patients with stable and unstable angina [57]. Inhibition of CPT-I and the subsequent facilitation of carbohydrate oxidation as well as elevation of pH may suppress osteogenic differentiation of muscle cells with unknown mechanisms. In FOP patients, major and minor muscle injuries often facilitate HO. Platelet aggregation at the site of trauma is possibly involved in the formation of HO, which can be potentially suppressed by perhexiline. Although mice taking perhexiline showed moderate reduction in the volume of HO, further studies are required to test whether lower concentrations of perhexiline exert a sufficient effect to ameliorate HO in humans.

Acknowledgments We thank Dr. Morio Kawamura at Nagoya University School of Health Science for productive discussion with us on our studies, and Ms. Keiko Itano for her technical assistance. This study was supported by Grants-in-Aid from the Ministry of Education, Culture, Sports, Science, and Technology of Japan, and the Ministry of Health, Labor, and Welfare of Japan.

Conflict of interest The authors have no conflict of interest and nothing to disclose.

References

1. Kaplan FS, Le Merrer M, Glaser DL, Pignolo RJ, Goldsby RE, Kitterman JA, Groppe J, Shore EM (2008) Fibrodysplasia ossificans progressiva. Best Pract Res Clin Rheurmatol 22:191–205
2. Glaser DL, Rocke DM, Kaplan FS (1998) Catastrophic falls in patients who have fibrodysplasia ossificans progressiva. Clin Orthop Relat Res 346:110–116
3. Rogers JG, Geho WB (1979) Fibrodysplasia ossificans progressiva. A survey of forty-two cases. J Bone Joint Surg Am 61:909–914
4. Connor JM, Evans DA (1982) Fibrodysplasia ossificans progressiva. The clinical features and natural history of 34 patients. J Bone Joint Surg Br 64:76–83
5. Lanchoney TF, Cohen RB, Rocke DM, Zasloff MA, Kaplan FS (1995) Permanent heterotopic ossification at the injection site after diphtheria–tetanus–pertussis immunizations in children who have fibrodysplasia ossificans progressiva. J Pediatr 126:762–764
6. Kitterman JA, Kantanie S, Rocke DM, Kaplan FS (2005) Iatrogenic harm caused by diagnostic errors in fibrodysplasia ossificans progressiva. Pediatrics 116:e654–e661
7. Kawai T, Urist MR (1988) Quantitative computation of induced heterotopic bone formation by an image analysis system. Clin Orthop Relat Res 233:262–267
8. Hayashi T, Kawai T, Ishikawa A, Kawai H, Nakano K, Takei Y, Kuroki K (2008) Histological analysis of induced cartilage on the biodegradable or nonbiodegradable membranes from immature muscular tissue in vitro. J Biomed Mater Res A 86:1048–1054
9. Shore EM, Xu M, Feldman GJ, Fenstermacher DA, Cho TJ, Choi IH, Connor JM, Delai P, Glaser DL, LeMerrer M, Morhart R, Rogers JG, Smith R, Triffitt JT, Urtizberea JA, Zasloff M, Brown MA, Kaplan FS (2006) A recurrent mutation in the BMP type I receptor ACVR1 causes inherited and sporadic fibrodysplasia ossificans progressiva. Nat Genet 38:525–527
10. DiCesare PE, Nimni ME, Peng L, Yazdi M, Cheung DT (1991) Effects of indomethacin on demineralized bone-induced heterotopic ossification in the rat. J Orthop Res 9:855–861
11. Zhang X, Schwarz EM, Young DA, Puzas JE, Rosier RN, O'Keefe RJ (2002) Cyclooxygenase-2 regulates mesenchymal cell differentiation into the osteoblast lineage and is critically involved in bone repair. J Clin Invest 109:1405–1415
12. Rogers JG, Dorst JP, Geho WB (1977) Use and complications of high-dose disodium etidronate therapy in fibrodysplasia ossificans progressiva. J Pediatr 91:1011–1014
13. Brantus JF, Meunier PJ (1998) Effects of intravenous etidronate and oral corticosteroids in fibrodysplasia ossificans progressiva. Clin Orthop Relat Res 346:117–120
14. Gannon FH, Glaser D, Caron R, Thompson LD, Shore EM, Kaplan FS (2001) Mast cell involvement in fibrodysplasia ossificans progressiva. Hum Pathol 32:842–848
15. Kaplan FS, Tabas JA, Gannon FH, Finkel G, Hahn GV, Zasloff MA (1993) The histopathology of fibrodysplasia ossificans progressiva. An endochondral process. J Bone Joint Surg Am 75: 220–230
16. Kaplan FS, Glaser DL, Shore EM, Pignolo RJ, Xu M, Zhang Y, Senitzer D, Forman SJ, Emerson SG (2007) Hematopoietic stem-cell contribution to ectopic skeletogenesis. J Bone Joint Surg Am 89:347–357
17. Glaser DL, Kaplan FS (2005) Treatment considerations for the management of fibrodysplasia ossificans progressiva. Clin Rev Bone Miner Metab 3:243–250
18. Yu PB, Hong CC, Sachidanandan C, Babitt JL, Deng DY, Hoyng SA, Lin HY, Bloch KD, Peterson RT (2008) Dorsomorphin inhibits BMP signals required for embryogenesis and iron metabolism. Nat Chem Biol 4:33–41
19. Yu PB, Deng DY, Lai CS, Hong CC, Cuny GD, Bouxsein ML, Hong DW, McManus PM, Katagiri T, Sachidanandan C, Kamiya N, Fukuda T, Mishina Y, Peterson RT, Bloch KD (2008) BMP type I receptor inhibition reduces heterotopic [corrected] ossification. Nat Med 14:1363–1369
20. Shimono K, Tung WE, Macolino C, Chi AH, Didizian JH, Mundy C, Chandraratna RA, Mishina Y, Enomoto-Iwamoto M, Pacifici M, Iwamoto M (2011) Potent inhibition of heterotopic ossification by nuclear retinoic acid receptor-gamma agonists. Nat Med 17:454–460
21. Heemskerk J, Tobin AJ, Bain LJ (2002) Teaching old drugs new tricks. Meeting of the Neurodegeneration Drug Screening Consortium, 7–8 April 2002, Washington, DC, USA. Trends Neurosci 25:494–496
22. Abbott A (2002) Neurologists strike gold in drug screen effort. Nature 417:109
23. Katagiri T, Imada M, Yanai T, Suda T, Takahashi N, Kamijo R (2002) Identification of a BMP-responsive element in Id1, the gene for inhibition of myogenesis. Genes Cells 7:949–960
24. Katagiri T, Yamaguchi A, Komaki M, Abe E, Takahashi N, Ikeda T, Rosen V, Wozney JM, Fujisawa-Sehara A, Suda T (1994) Bone morphogenetic protein-2 converts the differentiation pathway of C2C12 myoblasts into the osteoblast lineage. J Cell Biol 127:1755–1766
25. Kodaira K, Imada M, Goto M, Tomoyasu A, Fukuda T, Kamijo R, Suda T, Higashio K, Katagiri T (2006) Purification and identification of a BMP-like factor from bovine serum. Biochem Biophys Res Commun 345:1224–1231
26. Kawakami T, Uji H, Antoh M, Hasegawa H, Kise T, Eda S (1993) Squalane as a possible carrier of bone morphogenetic protein. Biomaterials 14:575–577
27. Boergermann JH, Kopf J, Yu PB, Knaus P (2010) Dorsomorphin and LDN-193189 inhibit BMP-mediated Smad, p38 and Akt signalling in C2C12 cells. Int J Biochem Cell Biol 42:1802–1807
28. Rothstein JD, Patel S, Regan MR, Haenggeli C, Huang YH, Bergles DE, Jin L, Dykes Hoberg M, Vidensky S, Chung DS, Toan SV, Bruijn LI, Su ZZ, Gupta P, Fisher PB (2005) Beta-lactam antibiotics offer neuroprotection by increasing glutamate transporter expression. Nature 433:73–77
29. Vincent AM, Sakowski SA, Schuyler A, Feldman EL (2008) Strategic approaches to developing drug treatments for ALS. Drug Discov Today 13:67–72
30. Gerber AN, Masuno K, Diamond MI (2009) Discovery of selective glucocorticoid receptor modulators by multiplexed reporter screening. Proc Natl Acad Sci USA 106:4929–4934
31. Sleigh JN, Buckingham SD, Esmaeili B, Viswanathan M, Cuppen E, Westlund BM, Sattelle DB (2011) A novel Caenorhabditis elegans allele, smn-1(cb131), mimicking a mild form of spinal muscular atrophy, provides a convenient drug screening platform highlighting new and pre-approved compounds. Hum Mol Genet 20:245–260
32. Bayer R, Mannhold R (1987) Fendiline: a review of its basic pharmacological and clinical properties. Pharmatherapeutica 5:103–136
33. Nawrath H, Klein G, Rupp J, Wegener JW, Shainberg A (1998) Open state block by fendiline of L-type Ca++ channels in ventricular myocytes from rat heart. J Pharmacol Exp Ther 285:546–552
34. Orosz F, Christova TY, Ovadi J (1988) Functional in vitro test of calmodulin antagonism: effect of drugs on interaction between calmodulin and glycolytic enzymes. Mol Pharmacol 33:678–682
35. Nagano N (2006) Pharmacological and clinical properties of calcimimetics: calcium receptor activators that afford an innovative approach to controlling hyperparathyroidism. Pharmacol Ther 109:339–365

36. Nemeth EF, Steffey ME, Hammerland LG, Hung BC, Van Wagenen BC, DelMar EG, Balandrin MF (1998) Calcimimetics with potent and selective activity on the parathyroid calcium receptor. Proc Natl Acad Sci USA 95:4040–4045
37. Wada M, Nagano N (2003) Control of parathyroid cell growth by calcimimetics. Nephrol Dial Transpl 18(Suppl 3):iii13–iii17
38. Watanabe H, Takahashi R, Tran QK, Takeuchi K, Kosuge K, Satoh H, Uehara A, Terada H, Hayashi H, Ohno R, Ohashi K (1999) Increased cytosolic Ca(2+) concentration in endothelial cells by calmodulin antagonists. Biochem Biophys Res Commun 265:697–702
39. Cheng JS, Chou KJ, Wang JL, Lee KC, Tseng LL, Tang KY, Huang JK, Chang HT, Su W, Law YP, Jan CR (2001) Fendiline mobilizes intracellular Ca2+ in Chang liver cells. Clin Exp Pharmacol Physiol 28:729–733
40. Wang J, Cheng J, Chan R, Tseng L, Chou K, Tang K, Chung Lee K, Lo Y, Jan C (2001) The anti-anginal drug fendiline increases intracellular Ca(2+) levels in MG63 human osteosarcoma cells. Toxicol Lett 119:227–233
41. Lin MC, Jan CR (2002) The anti-anginal drug fendiline elevates cytosolic Ca(2+) in rabbit corneal epithelial cells. Life Sci 71:1071–1079
42. Jorgensen NR (2005) Short-range intercellular calcium signaling in bone. APMIS Suppl 118:5–36
43. Spangler JG (2008) Bone biology and physiology: implications for novel osteoblastic osteosarcoma treatments? Med Hypotheses 70:281–286
44. Lindberg JS (2005) Calcimimetics: a new tool for management of hyperparathyroidism and renal osteodystrophy in patients with chronic kidney disease. Kidney Int Suppl 67: S33–S36
45. Zerbi S, Ruggiero P, Pedrini LA (2008) Massive soft tissue calcifications and cinacalcet. J Clin Endocrinol Metab 93:1121–1122
46. Mohammed IA, Sekar V, Bubtana AJ, Mitra S, Hutchison AJ (2008) Proximal calciphylaxis treated with calcimimetic 'Cinacalcet'. Nephrol Dial Transpl 23:387–389
47. Shah RR, Oates NS, Idle JR, Smith RL, Lockhart JD (1982) Impaired oxidation of debrisoquine in patients with perhexiline neuropathy. Br Med J 284:295–299
48. Sallustio BC, Westley IS, Morris RG (2002) Pharmacokinetics of the antianginal agent perhexiline: relationship between metabolic ratio and steady-state dose. Br J Clin Pharmacol 54:107–114
49. Fardeau M, Tome FM, Simon P (1979) Muscle and nerve changes induced by perhexiline maleate in man and mice. Muscle Nerve 2:24–36
50. Morgan MY, Reshef R, Shah RR, Oates NS, Smith RL, Sherlock S (1984) Impaired oxidation of debrisoquine in patients with perhexiline liver injury. Gut 25:1057–1064
51. Horowitz JD, Sia ST, Macdonald PS, Goble AJ, Louis WJ (1986) Perhexiline maleate treatment for severe angina pectoris—correlations with pharmacokinetics. Int J Cardiol 13:219–229
52. Cole PL, Beamer AD, McGowan N, Cantillon CO, Benfell K, Kelly RA, Hartley LH, Smith TW, Antman EM (1990) Efficacy and safety of perhexiline maleate in refractory angina. A double-blind placebo-controlled clinical trial of a novel antianginal agent. Circulation 81:1260–1270
53. Inglis S, Stewart S (2006) Metabolic therapeutics in angina pectoris: history revisited with perhexiline. Eur J Cardiovasc Nurs 5:175–184
54. Fleckenstein-Grun G, Fleckenstein-Grun A, Byon YK, Kem KW 1978 Mechanisms of action of Ca++ antagonists in the treatment of coronary disease, with special reference to perhexiline maleate. In: Perhexiline Maleate Proceedings of a Symposium, pp 1–22
55. Kennedy JA, Unger SA, Horowitz JD (1996) Inhibition of carnitine palmitoyltransferase-1 in rat heart and liver by perhexiline and amiodarone. Biochem Pharmacol 52:273–280
56. Stanley WC (2002) Partial fatty acid oxidation inhibitors for stable angina. Expert Opin Invest Drug 11:615–629
57. Willoughby SR, Stewart S, Chirkov YY, Kennedy JA, Holmes AS, Horowitz JD (2002) Beneficial clinical effects of perhexiline in patients with stable angina pectoris and acute coronary syndromes are associated with potentiation of platelet responsiveness to nitric oxide. Eur Heart J 23:1946–1954

J Bone Miner Metab (2013) 31:34–43
DOI 10.1007/s00774-012-0381-1

ORIGINAL ARTICLE

Identification of a novel bone morphogenetic protein (BMP)-inducible transcript, BMP-inducible transcript-1, by utilizing the conserved BMP-responsive elements in the Id genes

Masashi Shin · Satoshi Ohte · Toru Fukuda · Hiroki Sasanuma · Katsumi Yoneyama · Shoichiro Kokabu · Arei Miyamoto · Sho Tsukamoto · Hirohiko Hohjoh · Eijiro Jimi · Takenobu Katagiri

Received: 23 January 2012 / Accepted: 25 July 2012 / Published online: 14 September 2012

Abstract Bone morphogenetic proteins (BMPs) inhibit myogenesis and induce osteoblastic differentiation in myoblasts. They also induce the transcription of several common genes, such as Id1, Id2 and Id3, in various cell types. We have reported that a GC-rich element in the Id1 gene functions as a BMP-responsive element (BRE) that is regulated by Smads. In this study, we analyzed and identified BREs in the 5′-flanking regions of the mouse Id2 and Id3 genes. The core GGCGCC sequence was conserved among the BREs in the Id1, Id2 and Id3 genes and was essential for the response to BMP signaling via Smads. We found a novel BRE on mouse chromosome 13 at position 47,723,740–47,723,768 by searching for conserved sequences containing the Id1 BRE. This potential BRE was found in the 5′-flanking region of a novel gene that produces a non-coding transcript, termed BMP-inducible transcript-1 (BIT-1), and this element regulated the expression of this gene in response to BMP signaling. We found that BIT-1 is expressed in BMP target tissues such as the testis, brain, kidney and cartilage. These findings suggest that the transcriptional induction of the Ids, BIT-1 and additional novel genes containing the conserved BRE sequence may play an important role in the regulation of the differentiation and/or function of target cells in response to BMPs.

Keywords Bone morphogenetic proteins (BMPs) · Id · Transcription

Electronic supplementary material The online version of this article (doi:10.1007/s00774-012-0381-1) contains supplementary material, which is available to authorized users.

M. Shin · S. Ohte · T. Fukuda · H. Sasanuma · K. Yoneyama · S. Kokabu · A. Miyamoto · S. Tsukamoto · T. Katagiri (✉)
Division of Pathophysiology, Research Center for Genomic Medicine, Saitama Medical University, 1397-1 Yamane, Hidaka-shi, Saitama 350-1241, Japan
e-mail: katagiri@saitama-med.ac.jp

H. Hohjoh
Department of Molecular Pharmacology, National Institute of Neuroscience, NCNP, Kodaira, Tokyo 187-8502, Japan

E. Jimi
Department of Biosciences, Kyushu Dental College, Kitakyushu-shi, Fukuoka 803-8580, Japan

Introduction

Bone morphogenetic proteins (BMPs) are multifunctional growth factors that are members of the transforming growth factor-β family [1]. They exhibit unique activity in bone matrix that is characterized by ectopic bone formation in muscle tissues in vivo [2]. BMPs inhibit the myogenic differentiation of myoblasts and induce osteogenic differentiation into osteoblastic lineage cells in vitro [3]. They physiologically regulate not only bone formation but also the development and regeneration of various tissues in vertebrates and lower animals [4].

BMP signaling is transduced by two different transmembrane serine/threonine kinase receptors—the type I and type II receptors [5, 6]. The BMP-bound type II receptor kinase phosphorylates the type I receptor. The activated BMP type I receptor kinase subsequently phosphorylates a serine–valine–serine motif at the C-termini of Smad1, Smad5 and Smad8, which are BMP receptor-regulated Smads (R-Smads). The phosphorylated R-Smads form heteromeric complexes with Smad4 and translocate into the nucleus to directly regulate the transcription of target genes.

The Id family members are negative regulators of myogenesis that have a common helix–loop–helix structure, and their genes have been shown to be typical early response genes of BMP signaling in various cell types [7–9]. A GC-rich 29-bp element in the 5′ enhancer region of the Id1 gene was identified as the BMP-responsive element (BRE), which is recognized by a complex of Smad1/5 and Smad4 in response to the activation of the BMP type I receptor [7]. Mad, a *Drosophila* homolog of mammalian Smad1, also binds to a GC-rich sequence in target genes [10, 11]. Additional GC-rich elements have been found in the target genes of BMPs [10–14].

In the present study, we analyzed functional BREs in the mouse Id2 and Id3 genes. We identified the conserved GGCGCC sequence in the BREs of the Id1-Id3 genes, which are recognized by Smad1 and Smad4 in response to BMP-4. Moreover, we found a novel BRE by searching the mouse genome for a region homologous to the Id1 BRE. This novel BRE regulates the transcription of a novel non-coding BMP-inducible transcript, termed BIT-1, that is mainly expressed in the testis, brain, kidney and cartilage in mice.

Materials and methods

Plasmid constructs

To construct the luciferase reporter plasmids, 3.1-, 5.7- and 0.8-kb fragments from the 5′ regions of the mouse Id2 and Id3 genes and BIT-1, respectively, were inserted between the KpnI and EcoRV sites of pGL4.14 (Promega, Madison, WI, USA) by a standard polymerase chain reaction (PCR) method using PrimeStar HS DNA polymerase (TaKaRa, Shiga, Japan) with mouse genomic DNA as a template. The primer sequences were as follows: 5′-atggtaccCTTCTGCC AAGGAAGAGTTC-3′ (mId2-5KpnI), 5′-atgatatcACCAG GCTCGGTTCAGAATG-3′ (mId2-3EcoRV), 5′-atggtaccG AGTGCTGAGACTGTTAAGTAT-3′ (mId3-5KpnI), 5′-at gatatcCCTAAAGCAAACAGTGC-3′ (mId3-3EcoRV), 5′-atggtaccGCACAAGTAGTTATGGAGAC-3′ (BIT-1-5KpnI) and 5′-atgatatcACAGAACCTCGGAGACTGAC-3′ (BIT-1-3EcoRV) (lowercase letters indicate the flanking sequence). Deletion mutants were generated by PCR using each specific upper primer and the mId2-3EcoRV and mId3-3EcoRV primers with Id2(3.1)-luc and Id3(5.7)-luc as templates, respectively. To generate Id2WT4F-luc, Id3WT4F-luc, Id2WT4R-luc, Id3WT4R-luc, Id2MUT4F-luc, Id3MUT4F-luc and the novel BREWT4F-luc, four tandem repeats of the specific wild-type or mutant DNA sequences of the 34-bp Id2 BRE, 35-bp Id3 BRE or 29-bp novel BRE were synthesized (TaKaRa). These repeat sequences were then subcloned into the HindIII recognition site of pGL4.26 (Promega). The sequences of the BREs are as follows: 5′-TTGCTATGGCAGCCGCCTGAGCGGCG CCGCGAGG-3′ (Id2WT), 5′-TTGCTATGGCAGCCGCC TGAGCTTTGCCGCGAGG-3′ (Id2MUT), 5′-ATGACGTC CCACCCTGGCGCCAGGCTGTCTGGGGC-3′ (Id3WT), 5′-ATGACGTCCCACCCTTTTGCCAGGCTGTCTGGGG C-3′ (Id3MUT) and 5′-CAGAGCGACCGCCCGGCCGGC GCCAGCAG-3′ (novel BRE) (the underlined regions indicate mutations). Id2-2867MUT-luc and Id3-3304MUT-luc were constructed via a standard PCR technique using the following primers: 5′-CAGCCGCCTGAGCTTTGCCG CGAGGACAAG-3′ (Id2-2867MUT-luc sense), 5′-CTTG TCCTCGCGGCAAAGCTCAGGCGGCTG-3′ (Id2-2867 MUT-luc anti-sense), 5′-CGTCCCACCCTTTTGCCAGG CTGTCTGGGG-3′ (Id3-3303MUT-luc sense) and 5′-CCC CAGACAGCCTGGCAAAAGGGTGGGACG-3′ (Id3-330 3MUT-luc anti-sense). Mouse Smad1 and Smad4 expression vectors have been described previously [7]. Mouse Rp58 (GenBank ID 30928) was obtained using standard reverse transcriptase (RT)-PCR techniques with PrimeStar HS DNA polymerase (TaKaRa) and cloned into the pcDEF3 expression vector [15]. The DNA sequence of each construct was confirmed by DNA sequencing using an ABI3500 Genetic Analyzer (Applied Biosystems, Foster City, CA, USA).

Cell culture, transfection and luciferase assay

C2C12 mouse myoblasts were maintained as previously described [3]. Primary osteoblasts were prepared from newborn mouse calvaria as described previously [16]. Cells in a 96-well plate were transfected with 200 ng/well of plasmid DNA using 0.5 μl/well of Lipofectamine 2000 (Invitrogen, Carlsbad, CA, USA) as described previously [7]. The luciferase reporter assay was performed using the Dual-Glo Luciferase Assay system (Promega), luciferase reporter plasmids and phRL-SV40 (Promega) in the presence and absence of 10 ng/ml BMP-4 (R&D Systems, Minneapolis, MN, USA) with or without 100 nM LDN193189 (Stemgent, San Diego, CA, USA) for 24 h as previously described [7].

Electrophoretic mobility shift assay

Electrophoretic mobility shift assays (EMSAs) were performed as previously described [7, 17]. Oligonucleotides were labeled with the Biotin 3′ End DNA Labeling Kit (Thermo, Rockford, IL, USA). The DNA binding reaction was performed for 20 min at room temperature in 20 μl of binding buffer (10 mM Tris–HCl, pH 7.5; 50 mM KCl; 5 mM $MgCl_2$; 1 mM dithiothreitol; 0.05 % Nonidet P-40; 2.5 % glycerol), 1 μg of poly(dI-dC), 100 fmol of biotin-labeled DNA and 10 μg of nuclear extract proteins. For

supershift experiments, antibodies were added prior to the addition of the probe and incubated for 1 h at 4 °C. Antibodies against Smad1 (Invitrogen) and Smad4 (B-8; Santa Cruz Biotechnology, Santa Cruz, CA, USA) were used. For the competition experiments, the unlabeled double-stranded oligonucleotides were added to the mixtures at room temperature 30 min prior to the addition of the labeled probe. The sequences of the oligonucleotides used are as follows: 5′-CATGGCGACCGCCCGCGCGGCGCCAGC CT-3′ (Id1 wild-type BRE), 5′-CATGGCGACCGCCCGC GCTTTGCCAGCCT-3′ (Id1 mutant BRE), 5′-TTGCTAT GGCAGCCGCCTGAGCGGCGCCGCGAGG-3′ (Id2 wild-type BRE), 5′-TTGCTATGGCAGCCGCCTGAGCTTTG CCGCGAGG-3′ (Id2 mutant BRE), 5′-ATGACGTCCCA CCCTGGCGCCAGGCTGTCTGGGGC-3′ (Id3 wild-type BRE), 5′-ATGACGTCCCACCCTTTTGCCAGGCTGTC TGGGGC-3′ (Id3 mutant BRE) and 5′-CAGAGCGACCG CCCGGCCGGCGCCAGCAG-3′ (wild-type novel BRE) (the underlined regions indicate mutations). The samples were subjected to electrophoresis on a native 5 % acrylamide/0.5 × Tris-borate/EDTA gel and transferred to a nylon membrane. The biotin-labeled DNA was detected with the LightShift Chemiluminescent EMSA kit (Thermo).

Rapid amplification of cDNA ends

Rapid amplification of cDNA ends (3′ RACE) was performed using the 3′-Full RACE Core Set (TaKaRa). A library of adapter-ligated double-stranded cDNA was constructed from 1 μg of total RNA isolated from BMP-4-treated C2C12 cells according to the manufacturer's instructions. To isolate the 3′-end of the BIT-1 cDNA, primer 1 (5′-GCTGGGGGGTCAGTCTCCGA-3′) and primer 2 (5′-CTTCAAGACTCCTCCTGAGG-3′) were designed from the sequence of the 3′-region of BIT-1. PCR reactions were performed according to the manufacturer's instructions using AMV Reverse Transcriptase XL (TaKaRa). The PCR product was subcloned into T-Vector pMD20 (TaKaRa) and sequenced using an ABI3500 Genetic Analyzer (Applied Biosystems).

RT-PCR analysis

Total RNA was prepared using TRIzol Reagent (Invitrogen) and then reverse transcribed with SuperScript III reverse transcriptase (Invitrogen) according to the manufacturer's instructions. PCR reactions were performed with GoTaq (Promega). The primer sets used are as follows: 5′-GGGTGTTGCTGGACAGTGCC-3′ (BIT-1 sense), 5′-CACTACCCTGAGCACCACCC-3′ (BIT-1 anti-sense), 5′-TCCTGCAGCATGTAATCGAC-3′ (mouse Id1 sense), 5′-GAGAGGGTGAGGCTCTGTTG-3′ (mouse Id1 anti-sense), 5′-CTCCAAGCTCAAGGAACTGG-3′ (mouse Id2 sense), 5′-CGCAACCCACACAGAACTTA-3′ (mouse Id2 anti-sense), 5′-CTCTTGGACGACATGAACCAC-3′ (mouse Id3 sense), 5′-AGTGAGCTCAGCTGTCTGGAT-3′ (mouse Id3 anti-sense), 5′-GAGAGGGAAATCGTGCGTGA-3′ (mouse β-actin sense) and 5′-ACATCTGCTGGAAGGTGG AC-3′ (mouse β-actin anti-sense).

Chromatin immunoprecipitation

Chromatin immunoprecipitation (ChIP) was performed with a ChIP assay kit (Cell Signaling, Beverly, MA, USA) according to the manufacturer's instructions using antibodies against Smad1 (D59D7; Cell Signaling) and Smad4 (Cell Signaling). The purified DNA was analyzed by PCR using the following primers that detect sequences in the indicated promoter: 5′-TTCGCGCCCTAAGTCTGCAGG TG-3′ (Id1 promoter sense), 5′-AGGCCCGTGACGTCA CCCATTC-3′ (Id1 promoter anti-sense), 5′-CCTTGCAGG CATTGATCAGCTG-3′ (Id2 promoter sense), 5′-GAGCC CCGGAGCAGACTCTCT-3′ (Id2 promoter anti-sense), 5′-GCTATTCACAAGCCGCTCGCCG-3′ (Id3 promoter sense), 5′-GCCCAGCTGTGGGTCCGGGTCC-3′ (Id3 promoter anti-sense), 5′-CCAAGCCTTGTTGCCTGTGA ACG-3′ (BIT-1 promoter sense), and 5′-ACAGCTGATTC ATTGGCTCGGC-3′ (BIT-1 promoter anti-sense).

Statistical analysis

Comparisons were made using an unpaired Student's *t* test; the results are shown as the means ± SD. Statistical significance is indicated as $*p < 0.05$ and $**p < 0.01$.

Results

Identification of functional BREs in the mouse Id2 and Id3 genes

To examine the transcriptional mechanism of BMP early response genes, we analyzed the BREs in the mouse Id2 gene using a series of luciferase reporters harboring fragments of the 5′-flanking region of the mouse Id2 gene. For Id2(3.1)-luc, but not Id2(2.7)- or Id2(2.0)-luc, luciferase was induced in response to BMP-4 in C2C12 cells (Fig. 1a). The response to BMP-4 was dependent on the 34-bp region between positions −2867 and −2821 in the Id2 gene (5′-TTGCTATGGCAGCCGCCTGAGC**GGCG CC**GCGAGG-3′), which contains the GGCGCC sequence identified in the BRE of the Id1 gene (Fig. 1b) [7–9]. In both the forward and reverse orientations, the 34-bp region of the Id2 gene was sufficient to respond to BMP-4 (Fig. 1c). Moreover, mutation of GGCGCC to TTTGCC in the 34-bp region reduced the response to BMP-4 (Fig. 1d),

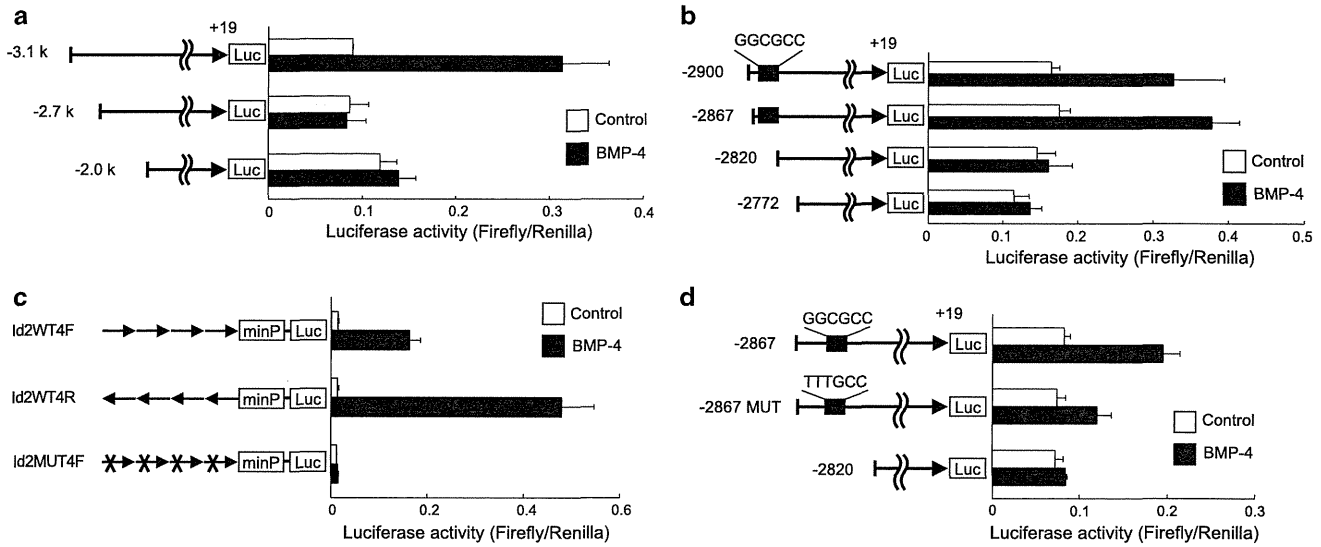

Fig. 1 Identification of a BRE in the mouse Id2 gene. **a** and **b** Deletion analysis of the 5′ region of the mouse Id2 gene in luciferase reporter constructs. Deletion constructs were generated from Id2(3.1)-luc. **c** Characterization of the 34-bp region of the mouse Id2 gene as a BMP-responsive enhancer. Reporter constructs harboring four copies of the 34-bp element with a wild-type or mutant sequence in the forward (Id2WT4F-luc and Id2MUT4F-luc) or reverse orientation (Id2WT4R-luc) were generated. **d** The role of the GGCGCC sequence of the Id2 BRE in the BMP response. The GGCGCC sequence in the BRE was substituted with TTTGCC in Id2(2867)-luc. Luciferase expression was determined in C2C12 cells in the presence and absence of 10 ng/ml BMP-4. Data are reported as the means ± SD ($n = 3$)

suggesting that the 34-bp region functions as the BRE in the Id2 gene.

Using the same strategy, we analyzed a BRE within a 5.7-kb 5′ -flanking region of the mouse Id3 gene (Fig. 2). The response of the Id3 gene to BMP-4 was highly dependent on the 35-bp region between positions −3299 and −3265 (5′-ATGACGTCCCACCCT**GGCGCC**AG-GCTGTCTGGGGC-3′), which also contains the GGCGCC sequence (Fig. 2a, b). Similar to the Id1 and Id2 genes, the GGCGCC sequence in the Id3 gene was both necessary and sufficient to mediate the response to BMP-4 (Fig. 2c, d), suggesting that this 35-bp region is the BRE in the Id3 gene.

Smad1 and Smad4 cooperatively induce the transcription of the Id2 and Id3 genes

Next, we analyzed the roles of Smad1 and Smad4 in the transcription of the Id2 and Id3 genes. Using EMSAs, we demonstrated that BMP-4 treatment induced the formation of a DNA–protein complex with both the Id2 and Id3 BREs (Fig. 3a, b). The DNA–protein complexes that formed with the BREs were supershifted upon the addition of antibodies against Smad1 and/or Smad4 (Fig. 3a, b). The DNA–protein complex that formed with the Id1 BRE was competed away by the addition of excess unlabeled DNA of not only the wild-type Id1 BRE but also the wild-type Id2 and Id3 BREs; however, the BREs with mutated GGCGCC sequences failed to compete (Fig. 3c). A ChIP assay demonstrated the binding of endogenous Smad1 and Smad4 to the BREs in the Id2 and Id3 genes in response to BMP-4 (Fig. 3d). The overexpression of Smad1 stimulated the expression of luciferase from both the Id2WT4F-luc reporter and the Id3WT4F-luc reporter (Fig. 3e, f). Co-transfection with Smad4 and Smad1 expression vectors enhanced luciferase expression in C2C12 cells (Fig. 3e, f).

Effects of Rp58 on the transcription of Id1, Id2 and Id3

Recently, Rp58 (*Zfp238*) was identified as a transcriptional repressor of Id2 and Id3 during myogenesis [18]. We examined the effect of the relationship between the Smads and Rp58 on the transcription of BMP-responsive genes, including Id1, Id2 and Id3, using luciferase reporter constructs driven by each native promoter/enhancer region [Id1(2.1)-luc, Id2(3.1)-luc and Id3(5.7)-luc, respectively]. As reported previously, the overexpression of Rp58 suppressed BMP-4-induced luciferase expression from Id2(3.1)-luc and Id3(5.7)-luc, but Rp58 did not suppress expression from Id1(2.1)-luc (Fig. 4a–c). The consensus sequences for Rp58 were located at positions +174 and +16 of the Id2 and Id3 BREs, respectively, but there was no Rp58 site in proximity to the Id1 BRE (Fig. 4d). An unexpected stimulation, rather than inhibition, of the Id1(2.1)-luc luciferase reporter by Rp58 was also observed with empty pGL4.26 vector (2.0-fold, data not shown).

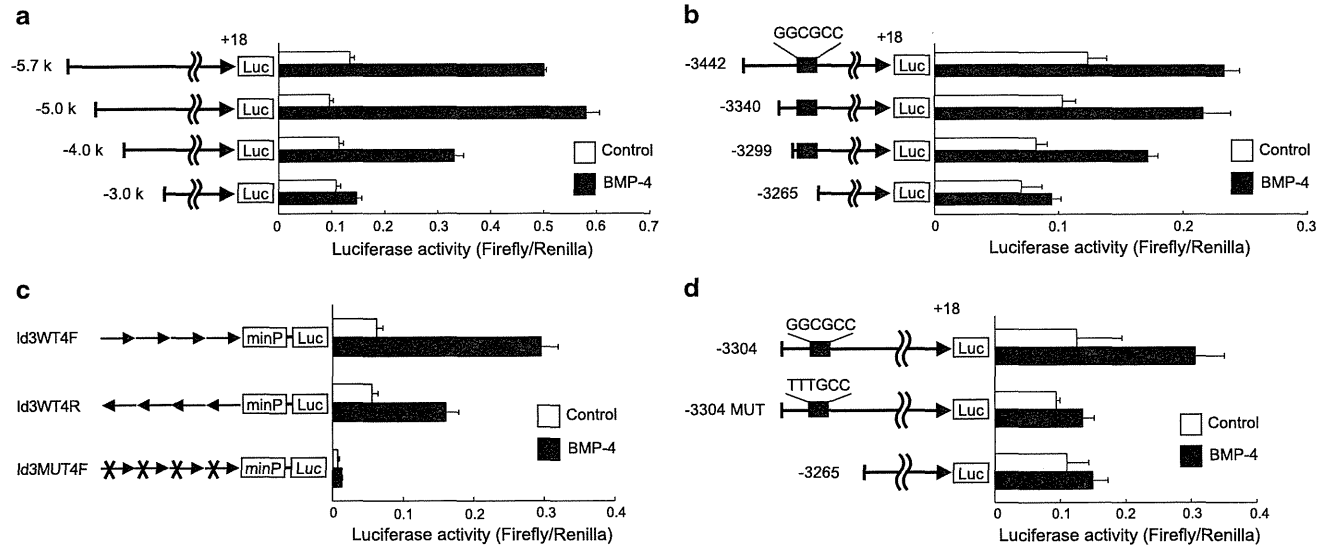

Fig. 2 Identification of a BRE in the mouse Id3 gene. **a** and **b** Deletion analysis of the 5′ region of the mouse Id3 gene in luciferase reporter constructs. Deletion constructs were generated from Id3(5.7)-luc. **c** Characterization of the 35-bp region of the mouse Id3 gene as a BMP-responsive enhancer. Reporter constructs containing four copies of the 35-bp element with a wild-type or mutant sequence in the forward (Id3WT4F-luc and Id3MUT4F-luc) or reverse orientation (Id3WT4R-luc) were constructed. **d** The role of the GGCGCC sequence of the Id3 BRE in the BMP response. The GGCGCC sequence in the BRE was substituted with TTTGCC in Id3(3304)-luc. Luciferase expression was determined in C2C12 cells in the presence and absence of 10 ng/ml BMP-4. Data are reported as the means ± SD ($n = 3$)

Identification of a novel BMP-responsive gene containing the conserved BRE

Due to the high level of conservation of the GC-rich BRE sequences among the Id1, Id2 and Id3 genes, we performed a BLAST (http://blast.ncbi.nim.njh.gov/Blast.cgi) search on the mouse genome to identify novel genes that have potential BREs. Using the Id1 BRE as the query sequence, we found a highly conserved sequence (23 of 29 bases identical) on chromosome 13 at position 47,723,740-47,723,768, which showed 79.3, 62 and 45 % homology with the BREs of Id1, Id2 and Id3, respectively (Fig. 5a). We generated a luciferase reporter construct containing four tandem copies of this potential novel BRE upstream of the minimal promoter (Fig. 5b). This reporter was activated in response to BMP-4, and this activation was suppressed by a chemical inhibitor of BMP receptors (Fig. 5b). Using EMSAs and ChIP assays, we demonstrated that this novel BRE was recognized by Smad1 and Smad4 in response to BMP-4 (Fig. 5c, d). Moreover, the overexpression of Smad1 in the presence of Smad4 induced luciferase expression in C2C12 cells (Fig. 5e).

A novel BMP-inducible transcript

Our findings suggest that the novel BRE regulates the transcription of an unidentified gene in response to BMP signaling. However, there were no genes that mapped within 10 kb of the novel BRE in the RefSeq database. We found that the novel BRE was located 255 bp upstream from a single cap analysis gene expression (CAGE) tag in the FANTOM database (TC ID T13F02D835DB; TU ID 83506 forward strand) (Fig. 6a, c). BMP-4 significantly stimulated luciferase expression from a reporter construct containing the genomic sequence from positions −805 to +49 relative to the CAGE tag, a region that includes the novel BRE, and this stimulation was suppressed by the BMP receptor inhibitor LDN-193189 (Fig. 6a). Furthermore, the corresponding endogenous transcript containing the CAGE tag, termed BIT-1, was induced in C2C12 cells within 30 min after treatment with BMP-4 (Fig. 6b). We determined the sequence of full-length BIT-1 from the CAGE tag in C2C12 cells cultured in the presence of BMP-4 using 3′ RACE (Fig. 6c). RT-PCR with a primer set that included the CAGE tag and the 3′ end sequence yielded the expected 1.0-kb single band, which was confirmed by direct DNA sequencing (Fig. 6d). The sequence data for BIT-1 have been deposited in the DDBJ/EMBL/GenBank databases under accession number AB679283. BIT-1 appears to be a non-coding RNA because the first open reading frame from the CAGE tag only encodes 6 amino acids and ATG codons do not correspond to the Kozak consensus sequence (Fig. 6c). Among the mouse tissues, BIT-1 was detected in the testis = brain > cartilage = kidney > and lung, in this order, and this expression pattern was quite different from that of other BMP-responsive

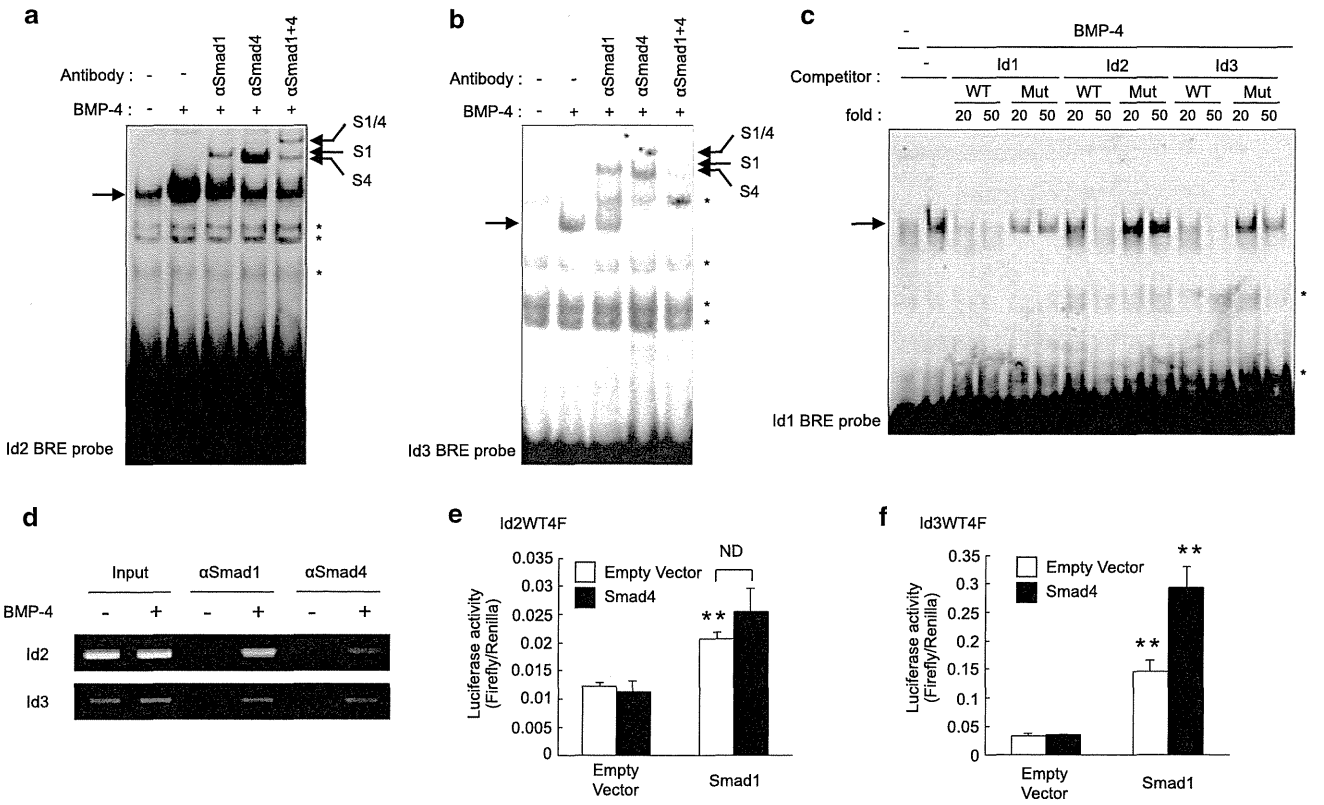

Fig. 3 Smad1 and Smad4 bind to BREs in the Id2 and Id3 genes. **a** and **b** The DNA–protein complexes formed with the Id2 and Id3 BREs contain Smad1 and Smad4. Nuclear extracts were prepared from C2C12 cells treated for 1 h with or without 100 ng/ml BMP-4. EMSAs were performed using the Id2 **a** or Id3 **b** BRE as a probe. Antibodies against Smad1 (S1) and Smad4 (S4) alone or in combination were added to the reaction mixtures. An *arrow from left to right* indicates BMP-induced complexes. *S1*, *S4* and *S1/S4* indicate supershifted bands with the indicated antibody. *Asterisks* indicate non-specific bands. **c** Sequence specificity of the BREs in the Id1, Id2 and Id3 genes. EMSAs were performed using nuclear extracts prepared from C2C12 cells treated with BMP-4 and the Id1 BRE as a probe. Excess unlabeled Id1, Id2 or Id3 BRE with a wild-type (WT) or mutant (Mut) GCCGCC sequence was added to the mixtures. An *arrow from left to right* indicates BMP-induced complexes. *Asterisks* indicate non-specific bands. **d** ChIP assays demonstrate that Smad1 and Smad4 bind to the Id2 and Id3 BREs in response to BMP-4 stimulation in C2C12 cells. **e** and **f** Smad1 and Smad4 activate the expression of Id2 and Id3 via BREs. Id2WT4F-luc **e** and Id3WT4F-luc **f** were co-transfected with Smad1 in the presence or absence of Smad4 in C2C12 cells. Data are reported as the means ± SD. ($n = 3$). $^{**}p < 0.01$ compared with cells transfected with empty vector and Smad1, Smad1 alone or Smad4 with Smad1

genes, such as Id1, Id2 and Id3 (Fig. 6e). Treatment with BMP-4 induced the expression of BIT-1 mRNA and the luciferase reporter not only in C2C12 cells but also in primary osteoblasts (Supplemental Fig. 1). We did not detect any changes in the induction of ALP activity, Id1WT4F-luc expression or the inhibition of myogenesis by BMP signaling with a transient transfection of C2C12 cells with BIT-1 cDNA (data not shown).

Discussion

In the present study, we analyzed the functional BREs in the mouse Id2 and Id3 genes, which are typical early response genes in BMP signaling. Both BREs were found in the 5′-flanking region of each gene; the Id2 BRE was located between positions −2854 and −2820, and the Id3 BRE was located between positions −3299 and −3625. Both mouse BREs were conserved at the corresponding positions in the human Id2 (97 %) and Id3 (100 %) genes (data not shown), suggesting that these regions are important for transcriptional regulation. The BREs in the Id1, Id2 and Id3 genes possess a highly conserved GGCGCC core sequence, and this sequence was recognized by a complex containing Smad1 and Smad4. We previously reported that mutation of the Id1 BRE from GGCGCC to TTTGCC destroys the response to BMP signaling by interrupting the binding of Smads to DNA [7].

Recently, other groups have also identified regions similar to the BREs in the mouse Id2 and human Id3 genes [19, 20]. ChIP-seq analysis using an antibody against Smad1/5 also identified two GC-rich Smad-binding elements in human endothelial cells, the GGCGCC sequence and a GGAGCC sequence [21]. Taken together, all of these

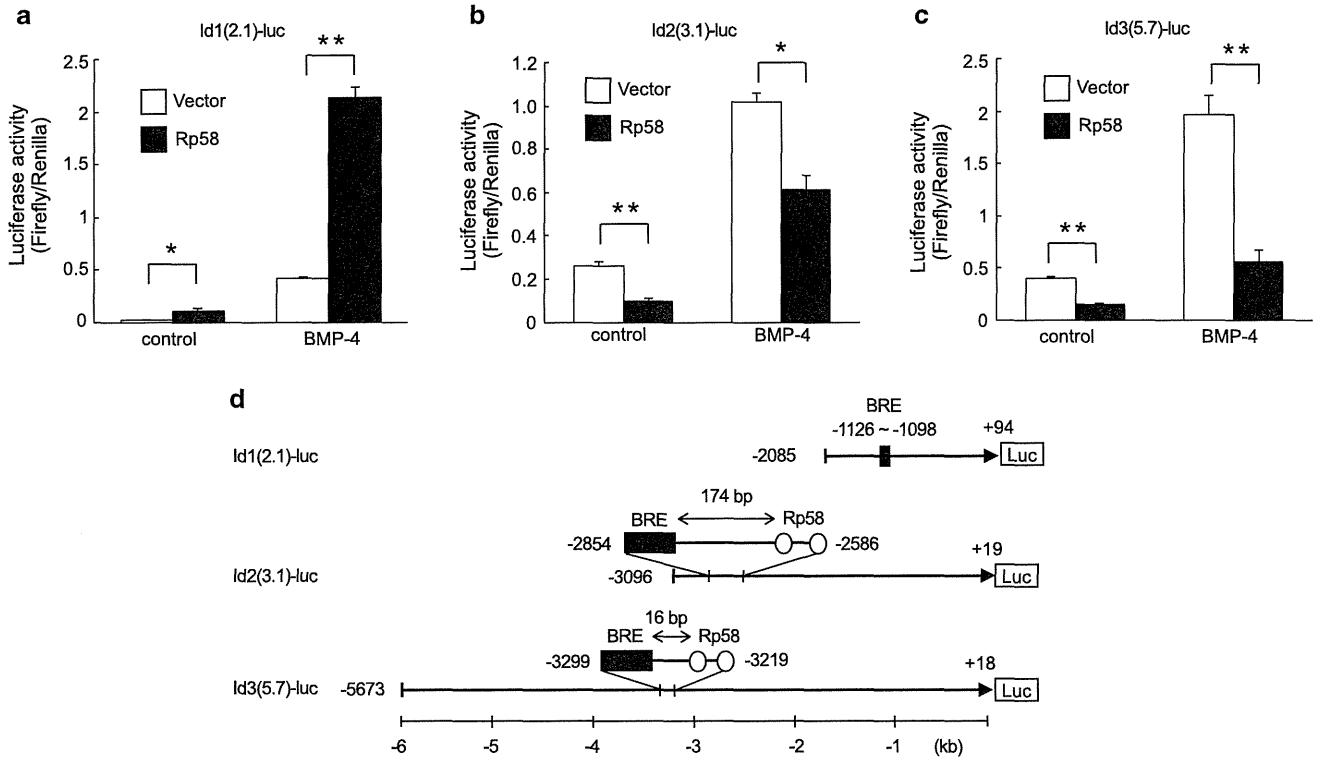

Fig. 4 Rp58 suppresses the expression of Id2 and Id3 but not of Id1. **a–c** Rp58 suppresses Id2(3.1)-luc **b** and Id3(5.7)-luc **c** but not Id1(2.1)-luc **a**. C2C12 cells were transfected with one of the reporter constructs with or without Rp58, and luciferase expression was determined in the presence or absence of BMP-4. Data are reported as the mean ± SD ($n = 3$). **d** A scheme of the relationship between the BREs (*solid squares*) and the Rp58 sites (*open circles*) in the Id1(2.1)-luc, Id2(3.1)-luc and Id3(5.7)-luc reporter constructs. $*p < 0.05$; $**p < 0.01$

findings indicate the importance of the GGCGCC sequence in the BMP response in mammalian cells. Interestingly, although two GGCGCC sequences were identified within a 60-bp region in the mouse Id2 gene, deleting only the region distal to the native promoter/enhancer abrogated the response to BMP-4. These results suggest that the GGCGCC sequence is essential, but not sufficient, for the BMP response. Additional sequences surrounding this core sequence may modify the binding affinity of Smads and/or other co-activators. Although a role for the CAGA (or complement GTCT) box in the BMP response has been suggested, our artificial BRE reporters, Id1WT4F-luc and Id2WT4F-luc, respond to BMP-4 although they lack the CAGA/GTCT box, suggesting that this element may not be essential for the response to BMP signaling. Additional studies are required to clarify the synergism between these sequences in BMP-regulated transcription.

We found a novel BMP-inducible transcript, BIT-1, by searching a genome database using the 29-bp Id1 BRE; the sequence was chosen because not only the core GGCGCC sequence but also the surrounding sequence may be required for the BMP response. The BIT-1 BRE exhibited the highest degree of homology with the Id1 BRE (79.3 %). BIT-1 seems to be one of the BMP-induced non-coding RNAs that include BMP/OP-resposive gene [22]. BIT-1 may have physiological roles in tissue development that are regulated by BMPs, as suggested by the fact that BIT-1 was found to be expressed in the target organs of BMPs, such as the testis, brain, kidney and cartilage. However, transient overexpression of the BIT-1 cDNA in C2C12 cells did not change the typical responses induced by BMPs, including alkaline phosphatase (ALP) activity, Id-luc expression or myogenesis (data not shown). Cell specificity may be involved in the functions of BIT-1. Gain-of-function and/or loss-of-function analyses in vivo will be required to elucidate the physiological roles of BIT-1. We have searched for novel BREs and BIT-1 in other species. Interestingly, whereas the novel BRE, including the GC-core sequence, is highly conserved not only in mouse but also in human, rat, orangutan, dog, horse and chicken, the conserved BIT-1 sequence is found in mouse and rat, but not in other species. This finding suggests that BIT-1 may function in rodents and that the conserved BRE in other species may regulate the expression of other transcripts in response to BMP signaling.

Recently, Rp58 has been identified as a transcriptional repressor of Id2 and Id3, which are negative regulators of the MyoD family of transcription factors [18]. The expression of Rp58 increased during myogenesis in C2C12

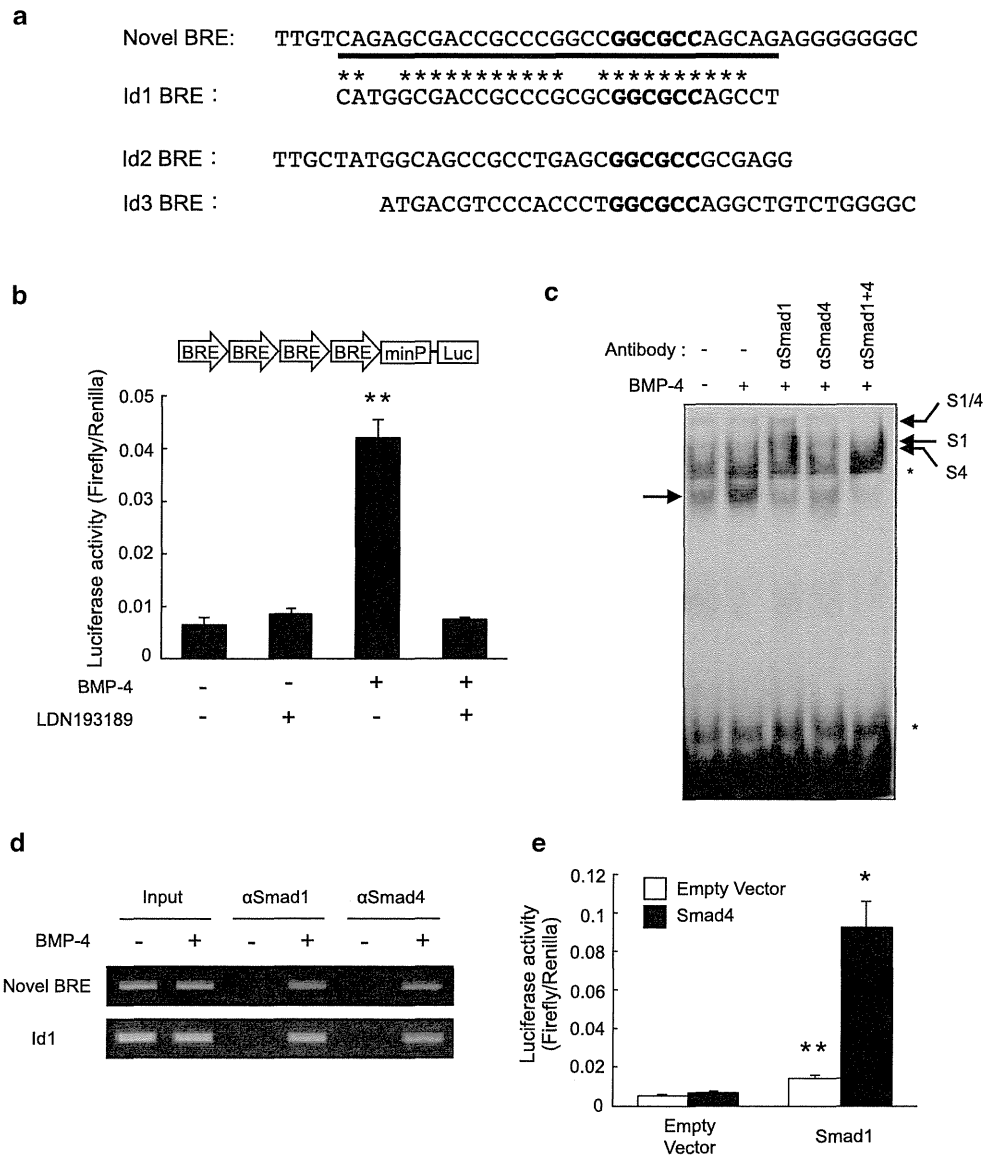

Fig. 5 Identification of a novel BRE in the mouse genome. **a** Comparison of the novel potential BRE with the BREs of Id1, Id2 and Id3. *Underlining* indicates the novel potential BRE identified in the mouse genome on chromosome 13 at position 47,723,740–47,723,768. Nucleotides that are conserved between the novel potential BRE and the Id1 BRE are indicated by *asterisks*. **b** Functional analysis of the novel BRE. A reporter construct containing four copies of the novel BRE was transfected into C2C12 cells, and luciferase expression was determined in the presence or absence of 10 ng/ml BMP-4 with or without 100 nM LDN193189. Data are reported as the means ± SD ($n = 3$). **c** Smad1 and Smad4 bind to the novel BRE. EMSAs were performed using the novel BRE as a probe and nuclear extracts of C2C12 cells treated with BMP-4. Antibodies against Smad1 or Smad4 were added to the mixture. An *arrow* indicates BMP-induced complexes. *S1*, *S4* and *S1/S4* indicate supershifted bands with the indicated antibody. *Asterisks* indicate non-specific bands. **d** ChIP assays demonstrate that Smad1 and Smad4 proteins bind to the novel BRE and the Id1 BRE in response to BMP-4 stimulation of C2C12 cells. **e** Smad1 and Smad4 induce the transcriptional activity of BRE. C2C12 cells were co-transfected with the 4× novel BRE luciferase reporter and Smad1 in the presence or absence of Smad4. Data are reported as the means ± SD ($n = 3$). $^{**}p < 0.01$ compared with cells transfected with empty vector and Smad1. $^{*}p < 0.05$ compared with cells transfected with Smad1 alone or with Smad4 and Smad1

cells [18]. We confirmed the finding that Rp58 suppressed the transcription of the Id2 and Id3 genes via the consensus sites in the 5′-flanking region of each gene. We observed that these Rp58 sites were located close to the BREs in both the Id2 and Id3 genes. The luciferase reporters lacking the Rp58 sites were not suppressed by the overexpression of Rp58, suggesting that Rp58 inhibits the transcription of Id2 and Id3 induced by BMP signaling by binding to the

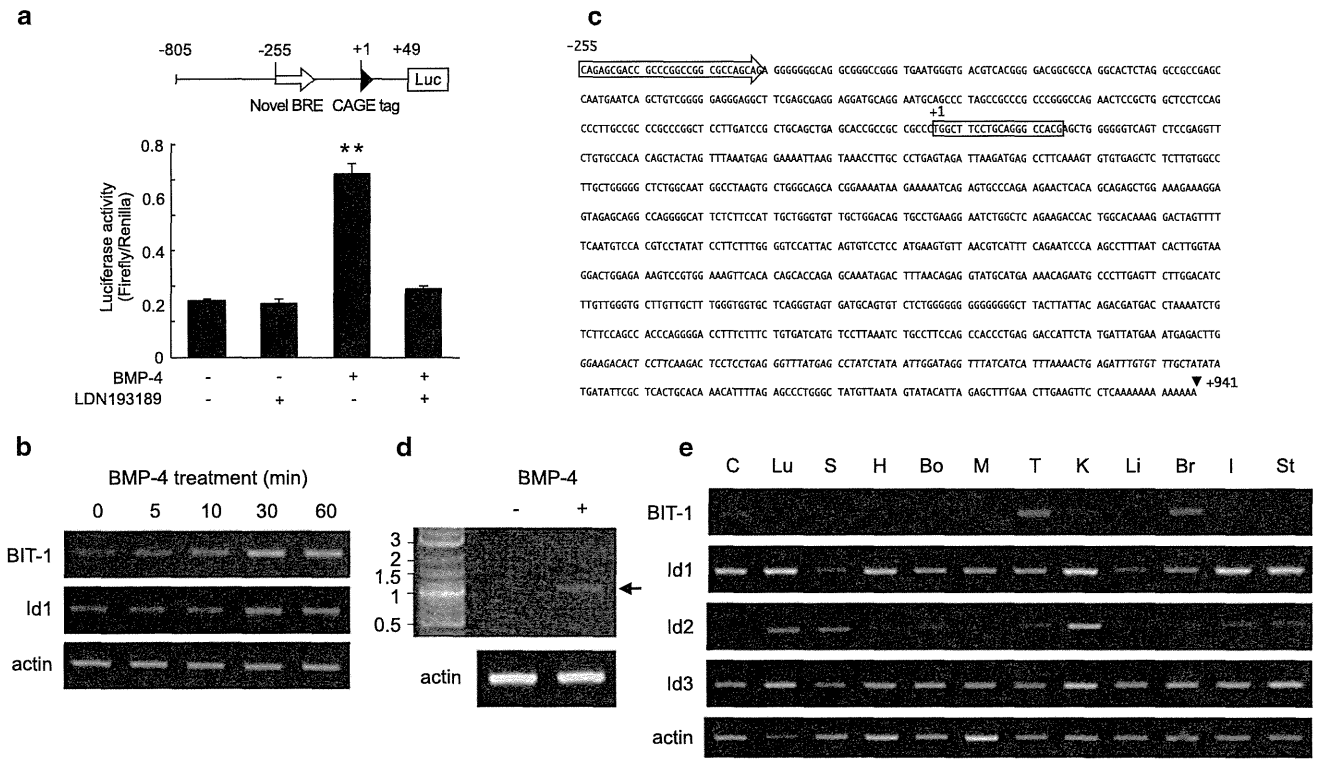

Fig. 6 The novel BRE regulates the transcription of BIT-1. **a** A luciferase reporter construct harboring the novel BRE was activated by BMP-4. A DNA fragment of mouse chromosome 13 position 47,723,190–47,724,044 containing the novel BRE (*open arrow*) and the CAGE tag (*triangle*) (−805 to +49) was cloned into the luciferase reporter vector pGL4.14 and transfected into C2C12 cells. Luciferase expression was determined in the presence or absence of BMP-4 with or without 100 nM LDN193189. Data are reported as the mean ± SD ($n = 3$). **b** RT-PCR analysis. C2C12 cells were treated with 100 ng/ml BMP-4 for the indicated time periods. The BIT-1, Id1 and actin mRNAs were amplified by RT-PCR. **c** Nucleotide sequence of the novel BRE and BIT-1. The novel BRE identified (*open arrow*), the CAGE tag (*open box*), and the 3′ end as determined by 3′ RACE (*solid triangle*) are indicated. The first nucleotide of the CAGE tag is denoted by +1. **d** Induction of BIT-1 by BMP-4 in C2C12 cells. The expected full-length BIT-1 was amplified by RT-PCR using primers that bind the CAGE tag and the 3′ end. **e** Expression of BIT-1, Id1, Id2 and Id3 in mouse tissues. RT-PCR analysis was performed using cDNA prepared from the following mouse tissues: *C* cartilage, *Lu* lung, *S* spleen, *H* heart, *Bo* bone, *M* muscle, *T* testis, *K* kidney, *Li* liver, *Br* brain, *I* intestine and *St* stomach. $^{**}p < 0.01$ compared with control

target promoter/enhancer regions. The molecular mechanism of this inhibition will be elucidated by analyzing the components that are recruited to the consensus site by Rp58.

In conclusion, we identified functional BREs in BMP early response genes containing the core GGCGCC sequence. A novel BMP-inducible transcript, BIT-1, may play a role in BMP-regulated tissue development.

Acknowledgments This work was supported in part by Health and Labour Sciences Research Grants for Research on Measures for Intractable Research from the Ministry of Health, Labour and Welfare of Japan, grants-in-aid from the Ministry of Education, Culture, Sports, Science and Technology (MEXT) of Japan, a grant-in-aid for the Supported Program for the Strategic Research Foundation at Private Universities from the MEXT (S0801004) and a grant-in-aid from the Takeda Science Foundation.

Conflict of interest All authors declare that they have no conflict of interest.

References

1. Attisano L, Wrana JL (2002) Signal transduction by the TGF-beta superfamily. Science 296:1646–1647
2. Urist MR (1965) Bone: formation by autoinduction. Science 150:893–899
3. Katagiri T, Yamaguchi A, Komaki M, Abe E, Takahashi N, Ikeda T, Rosen V, Wozney JM, Fujisawa-Sehara A, Suda T (1994) Bone morphogenetic protein-2 converts the differentiation pathway of C2C12 myoblasts into the osteoblast lineage. J Cell Biol 127:1755–1766
4. Katagiri T, Suda T, Miyazono K (2008) The bone morphogenetic proteins. In: Derynck R, Miyazono K (eds) TGF-β family. Cold Spring Harbor Press, New York, pp 121–149
5. Wan M, Cao X (2005) BMP signaling in skeletal development. Biochem Biophys Res Commun 328:651–657
6. Miyazono K, Maeda S, Imamura T (2005) BMP receptor signaling: transcriptional targets, regulation of signals, and signaling cross-talk. Cytokine Growth Factor Rev 16:251–263
7. Katagiri T, Imada M, Yanai T, Suda T, Takahashi N, Kamijo R (2002) Identification of a BMP-responsive element in Id1, the gene for inhibition of myogenesis. Genes Cells 7:949–960

8. Lopez-Rovira T, Chalaux E, Massague J, Rosa JL, Ventura F (2002) Direct binding of Smad1 and Smad4 to two distinct motifs mediates bone morphogenetic protein-specific transcriptional activation of Id1 gene. J Biol Chem 277:3176–3185
9. Korchynskyi O, ten Dijke P (2002) Identification and functional characterization of distinct critically important bone morphogenetic protein-specific response elements in the Id1 promoter. J Biol Chem 277:4883–4891
10. Kim J, Johnson K, Chen HJ, Carroll S, Laughon A (1997) Drosophila Mad binds to DNA and directly mediates activation of vestigial by Decapentaplegic. Nature 388:304–308
11. Xu X, Yin Z, Hudson JB, Ferguson EL, Frasch M (1998) Smad proteins act in combination with synergistic and antagonistic regulators to target Dpp responses to the Drosophila mesoderm. Genes Dev 12:2354–2370
12. Ishida W, Hamamoto T, Kusanagi K, Yagi K, Kawabata M, Takehara K, Sampath TK, Kato M, Miyazono K (2000) Smad6 is a Smad1/5-induced smad inhibitor. Characterization of bone morphogenetic protein-responsive element in the mouse Smad6 promoter. J Biol Chem 275:6075–6079
13. Kusanagi K, Inoue H, Ishidou Y, Mishima HK, Kawabata M, Miyazono K (2000) Characterization of a bone morphogenetic protein-responsive Smad-binding element. Mol Biol Cell 11:555–565
14. Karaulanov E, Knochel W, Niehrs C (2004) Transcriptional regulation of BMP4 synexpression in transgenic Xenopus. EMBO J 23:844–856
15. Goldman LA, Cutrone EC, Kotenko SV, Krause CD, Langer JA (1996) Modifications of vectors pEF-BOS, pcDNA1 and pcDNA3 result in improved convenience and expression. Biotechniques 21:1013–1015
16. Komaki M, Katagiri T, Suda T (1996) Bone morphogenetic protein-2 does not alter the differentiation pathway of committed progenitors of osteoblasts and chondroblasts. Cell Tissue Res 284:9–17
17. Shin M, Matsuo K, Tada T, Fukushima H, Furuta H, Ozeki S, Kadowaki T, Yamamoto K, Okamoto M, Jimi E (2011) The inhibition of RANKL/RANK signaling by osteoprotegerin suppresses bone invasion by oral squamous cell carcinoma cells. Carcinogenesis 32:1634–1640
18. Yokoyama S, Ito Y, Ueno-Kudoh H, Shimizu H, Uchibe K, Albini S, Mitsuoka K, Miyaki S, Kiso M, Nagai A, Hikata T, Osada T, Fukuda N, Yamashita S, Harada D, Mezzano V, Kasai M, Puri PL, Hayashizaki Y, Okado H, Hashimoto M, Asahara H (2009) A systems approach reveals that the myogenesis genome network is regulated by the transcriptional repressor RP58. Dev Cell 17:836–848
19. Nakahiro T, Kurooka H, Mori K, Sano K, Yokota Y (2011) Identification of BMP-responsive elements in the mouse Id2 gene. Biochem Biophys Res Commun 399:416–421
20. Shepherd TG, Theriault BL, Nachtigal MW (2008) Autocrine BMP4 signalling regulates ID3 proto-oncogene expression in human ovarian cancer cells. Gene 414:95–105
21. Morikawa M, Koinuma D, Tsutsumi S, Vasilaki E, Kanki Y, Heldin CH, Aburatani H, Miyazono K (2011) ChIP-seq reveals cell type-specific binding patterns of BMP-specific Smads and a novel binding motif. Nucleic Acids Res 39:8712–8727
22. Takeda K, Ichijo H, Fujii M, Mochida Y, Saitoh M, Nishitoh H, Sampath TK, Miyazono K (1998) Identification of a novel bone morphogenetic protein-responsive gene that may function as a noncoding RNA. J Biol Chem 273:17079–17085

DOI 10.1515/hsz-2012-0310 — Biol. Chem. 2013; 394(6): 703–714

Review

Takenobu Katagiri* and Sho Tsukamoto

The unique activity of bone morphogenetic proteins in bone: a critical role of the Smad signaling pathway

Abstract: Bone morphogenetic proteins (BMPs) are multifunctional cytokines that belong to the transforming growth factor-β family. BMPs were originally identified based on their unique activity, inducing heterotopic bone formation in skeletal muscle. This unique BMP activity is transduced by specific type I and type II transmembrane kinase receptors. Among the downstream pathways activated by these receptors, the Smad1/5/8 transcription factors appear to play critical roles in BMP activity. Smad1/5/8 transcription factors are phosphorylated at the C-terminal SVS motif by BMP type I receptors and then induce the transcription of early BMP-responsive genes by binding to conserved sequences in their enhancer regions. The linker regions of Smad1/5/8 contain multiple kinase phosphorylation sites, and phosphorylation and dephosphorylation of these sites regulate the transcriptional activity of Smad proteins. Gain-of-function mutations in one BMP type I receptor have been identified in patients with fibrodysplasia ossificans progressiva, a rare genetic disorder that is characterized by progressive heterotopic bone formation in the skeletal muscle. The mutant receptors activate the Smad signaling pathway even in the absence of BMPs, therefore novel inhibitors for the BMP receptor – Smad axis are being developed to prevent heterotopic bone formation in fibrodysplasia ossificans progressiva. Taken together, the data in the literature show that the BMP type I receptor – Smad signaling axis is the critical pathway for the unique activity of BMPs and is a potential therapeutic target for pathological conditions caused by inappropriate BMP activity.

Keywords: bone morphogenetic protein; dephosphorylation; phosphorylation; receptor; Smad.

***Corresponding author: Takenobu Katagiri,** Division of Pathophysiology, Research Center or Genomic Medicine, Saitama Medical University, 1397-1 Yamane, Hidaka-shi, Saitama 350-1241, Japan; and Project of Clinical and Basic Research for Fibrodysplasia Ossificans Progressiva at Saitama Medical University, 1397-1 Yamane, Hidaka-shi, Saitama 350-1241, Japan,
e-mail: katagiri@saitama-med.ac.jp

Sho Tsukamoto: Division of Pathophysiology, Research Center or Genomic Medicine, Saitama Medical University, 1397-1 Yamane, Hidaka-shi, Saitama 350-1241, Japan

Bone morphogenetic proteins and their role in bone formation

The discovery of bone morphogenetic protein

Bone morphogenetic protein (BMP) was originally discovered as a protein with heterotopic bone-inducing activity in the bone matrix (Urist, 1965; Reddi and Huggins, 1972). Marshall R. Urist (1965) observed the induction of new cartilage and bone with bone marrow in skeletal muscle after the implantation of bone matrix demineralized by treatment with hydrochloric acid. The demineralized bone matrix factor with this unique activity was named BMP because it was destroyed by digestion with trypsin (Urist and Strates, 1971). These findings also indicated that skeletal muscle and other soft tissues contain progenitor cells that are capable of differentiating into chondrocytes and osteoblasts under the control of BMP (Wosczyna et al., 2012). Other molecules, such as cytokines, hormones and small chemical compounds, do not show such bone-inducing activity, therefore this heterotopic bone induction is believed to be specific to BMP (Katagiri et al., 2008). The intracellular signal transduction downstream of BMP may play an important role in physiological and pathological bone formation (Miyazawa et al., 2002; Katagiri, 2010).

The structure – bioactivity relationship of bone morphogenetic proteins

In 1988, Wozney and colleagues obtained several peptide sequences from the bioactive 'BMP' fraction purified from

demineralized bovine bone matrix and successfully cloned four independent BMP cDNAs (BMP-1 through BMP-4; BMP-4 was originally called BMP-2b). The BMPs, except BMP-1, have strong homology with transforming growth factor-β1 (TGF-β1) and have been shown to be novel members of the TGF-β family (Wozney et al., 1988). Based on cDNA homology, more than 10 BMPs and related growth differentiation factors have also been identified in vertebrates (Figure 1) (Katagiri et al., 2008; Mueller and Nickel, 2012).

The members of the TGF-β family function as dimers (Sampath et al., 1990). Although bone matrix contains several types of BMPs, each recombinant BMP homodimer induces heterotopic cartilage, tendon and/or bone formation *in vivo*, suggesting that the original 'BMP' activity found in demineralized bone matrix represented the combined activity of heterogeneous BMPs (Rider and Mulloy, 2010). Furthermore, the overlapping expression of some BMP mRNAs during embryogenesis suggests a possibility of BMP heterodimer formation during skeletal development. BMP-2/BMP-6 and BMP-2/BMP-7 heterodimers show higher specific activity *in vitro* and *in vivo* than their respective homodimers (Israel et al., 1996; Valera et al., 2010; Buijs et al., 2012). BMP-1, a metalloproteinase, also induced heterotopic cartilage formation *in vivo*, though the molecular mechanisms underlying this activity remain unclear (Wozney et al., 1988). Dpp and 60A, BMP-2/4 and BMP-5/6/7 homologs in *Drosophila*, respectively, were capable of inducing heterotopic bone formation in rodents, even though flies do not have bone tissue

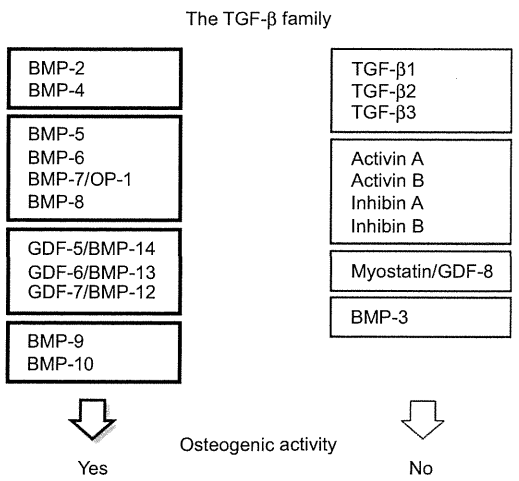

Figure 1 Osteogenic and non-osteogenic members of the TGF-β family.
Among the members of the TGF-β family examined their osteogenic activities, most BMPs are capable of inducing heterotopic bone formation when applied to skeletal muscle as recombinant proteins. In contrast, TGF-β proteins, activins, inhibins and BMP-3 do not have this activity.

(Sampath et al., 1993; Shimmi et al., 2005). A common intracellular signaling system activated by BMPs and homologs in vertebrates and flies may have different functions that are species- and cell type-dependent. Indeed, the TGF-β family members have multiple roles in proliferation, differentiation and apoptosis during embryonic development and in tissue maintenance and regeneration after birth (Giacomini et al., 2007; Wordinger and Clark, 2007; Katagiri et al., 2008; Miyazono et al., 2010; Cai et al., 2012; Otsuka et al., 2012). For example, BMP-9 has been shown to regulate blood glucose levels; a single subcutaneous injection of BMP-9 reduced the blood glucose levels in diabetic mice to near-normal levels (Chen et al., 2003). Moreover, some BMPs have been identified and/or purified from serum (Borovecki et al., 2004; Kodaira et al., 2006; Vukicevic and Grgurevic, 2009; Grgurevic et al., 2011). These findings suggest that BMPs act not only at the local but also the systemic level (Simic et al., 2006; Nemeth, 2008). The mechanisms that regulate the expression and activation of BMPs should be investigated further.

An *in vitro* model reflecting the unique activity of bone morphogenetic proteins

Heterotopic bone induction, one of the defining activities of BMPs, can be reproduced *in vitro*, at least in part, in C2C12 myoblasts derived from the thigh muscles of C3H mice (Blau et al., 1983). Similar to primary myoblasts, C2C12 cells proliferate as mononuclear cells and express *MyoD*, a master gene of skeletal muscle differentiation, but do not express muscle-contracting proteins, such as myosin heavy chain and troponin T. Terminal myogenic differentiation is induced upon entering G0. The treatment of C2C12 cells with osteogenic BMPs inhibits myogenic differentiation and induces an osteoblast differentiation phenotype, including high alkaline phosphatase activity and osteocalcin secretion (Katagiri et al., 1994). Similar effects were observed in primary myoblasts treated with BMPs (Katagiri et al., 1994). Although many types of hormones and cytokines inhibit the myogenesis of myoblasts *in vitro*, these molecules never induce osteoblastic differentiation in C2C12 cells (Katagiri et al., 2008). Furthermore, although TGF-β1 is known as a potent inhibitor of myogenesis, it does not induce osteoblastic differentiation in C2C12 cells *in vitro* or heterotopic bone formation *in vivo* (Sampath et al., 1987; Katagiri et al., 1994). Thus, an experimental model using C2C12 myoblasts may be a useful system for studying the unique intracellular signal transduction of BMPs *in vitro*. Indeed, Osterix, which is